Human TYK2 deficiency: Mycobacterial and viral infections without hyper-IgE syndrome

Alexandra Y. Kreins,[1,2] Michael J. Ciancanelli,[1*] Satoshi Okada,[1*] Xiao-Fei Kong,[1*] Noé Ramírez-Alejo,[1*] Sara Sebnem Kilic,[3**] Jamila El Baghdadi,[4**] Shigeaki Nonoyama,[5**] Seyed Alireza Mahdaviani,[6**] Fatima Ailal,[8**] Aziz Bousfiha,[8**] Davood Mansouri,[7**] Elma Nievas,[9**] Cindy S. Ma,[10,11] Geetha Rao,[10] Andrea Bernasconi,[12] Hye Sun Kuehn,[13] Julie Niemela,[13] Jennifer Stoddard,[13] Paul Deveau,[15,16] Aurelie Cobat,[15,16] Safa El Azbaoui,[4,17] Ayoub Sabri,[4,17] Che Kang Lim,[18,19] Mikael Sundin,[20] Danielle T. Avery,[10] Rabih Halwani,[21] Audrey V. Grant,[15,16] Bertrand Boisson,[1] Dusan Bogunovic,[1] Yuval Itan,[1] Marcela Moncada-Velez,[1,22] Ruben Martinez-Barricarte,[1] Melanie Migaud,[15,16] Caroline Deswarte,[15,16] Laia Alsina,[23,24,25] Daniel Kotlarz,[26] Christoph Klein,[26] Ingrid Muller-Fleckenstein,[27] Bernhard Fleckenstein,[27] Valerie Cormier-Daire,[28] Stefan Rose-John,[29] Capucine Picard,[1,15,16,30] Lennart Hammarstrom,[18***] Anne Puel,[15,16***] Saleh Al-Muhsen,[21***] Laurent Abel,[1,15,16***] Damien Chaussabel,[31***] Sergio D. Rosenzweig,[13,14***] Yoshiyuki Minegishi,[32***] Stuart G. Tangye,[10,11***] Jacinta Bustamante,[15,16,30***] Jean-Laurent Casanova,[1,15,16,33,34****] and Stéphanie Boisson-Dupuis[1,15,16****]

[1]St. Giles Laboratory of Human Genetics of Infectious Diseases, Rockefeller Branch, The Rockefeller University, New York, NY 10065
[2]Weill Cornell Graduate School of Medical Sciences, New York, NY 10065
[3]Department of Pediatric Immunology, Uludağ University Faculty of Medicine, 16059 Görükle, Bursa, Turkey
[4]Genetics Unit, Military Hospital Mohamed V, Hay Riad, 10100 Rabat, Morocco
[5]Department of Pediatrics, National Defense Medical College, Tokorozawa, Saitama 359-0042, Japan
[6]Pediatric Respiratory Diseases Research Center; and [7]Department of Clinical Immunology and Infectious Diseases, Masih Daneshvari Hospital; National Research Institute of Tuberculosis and Lung Diseases, Shahid Beheshti University of Medical Sciences, 141556153 Tehran, Iran
[8]Clinical Immunology Unit, Department of Pediatrics, King Hassan II University, CHU Ibn Rochd, 20000 Casablanca, Morocco
[9]Immunology Unit, Pediatric Hospital A. Fleming-OSEP, Mendoza 5500, Argentina
[10]Immunology Program, Garvan Institute of Medical Research, Darlinghurst, New South Wales 2010, Australia
[11]St. Vincent's Clinical School, University of New South Wales, Darlinghurst, New South Wales 2010, Australia
[12]Immunology and Rheumatology Service, Garrahan Hospital, Buenos Aires 1408, Argentina
[13]Department of Laboratory Medicine, Clinical Center; and [14]Primary Immunodeficiency Clinic, National Institute of Allergy and Infectious Diseases; National Institutes of Health, Bethesda, MD 20892
[15]Laboratory of Human Genetics of Infectious Diseases, Necker Branch, INSERM U1163, Necker Enfants Malades Hospital, 75015 Paris, France
[16]University Paris Descartes, Imagine Institute, 75006 Paris, France
[17]Faculty of Science-Kenitra, Ibn Tofaïl University, 14000 Kenitra, Morocco
[18]Division of Clinical Immunology, Department of Laboratory Medicine, Karolinska Institutet, Karolinska University Hospital Huddinge, 141 52 Stockholm, Sweden
[19]Department of Clinical Research, Singapore General Hospital, Singapore 169856
[20]Pediatric Hematology/Immunology, Astrid Lindgrens Children's Hospital and Karolinska Institutet, 141 86 Stockholm, Sweden
[21]Asthma Research Chair and Prince Naif Center for Immunology Research, Department of Pediatrics, College of Medicine, King Saud University, Riyadh 12372, Saudi Arabia
[22]Group of Primary Immunodeficiencies, Institute of Biology, University of Antioquia UdeA, 1226 Medellín, Colombia
[23]Baylor Institute for Immunology Research and [24]Baylor Research Institute, Dallas, TX 75204
[25]Allergy and Clinical Immunology Department, Hospital Sant Joan de Deu, Barcelona University, 08950 Barcelona, Spain
[26]Department of Pediatrics, Dr. von Hauner Children's Hospital, Ludwig Maximilians University, D-80337 Munich, Germany
[27]Institute of Clinical and Molecular Virology, University of Erlangen-Nuremberg, D-91054 Erlangen, Germany
[28]Department of Genetics, INSERM U1163, University Paris Descartes–Sorbonne Paris Cite, Imagine Institute, Necker Enfants Malades Hospital, 75015 Paris, France
[29]Institute of Biochemistry, University of Kiel, D-24098 Kiel, Germany
[30]Center for the Study of Primary Immunodeficiencies, Assistance Publique–Hôpitaux de Paris, Necker Enfants Malades Hospital, 75015 Paris, France
[31]Systems Biology Department, Sidra Medical and Research Center, Doha, Qatar
[32]Department of Immune Regulation, Graduate School, Tokyo Medical and Dental University, Bunkyo-ku, Tokyo 113-8510, Japan
[33]Pediatric Immunology and Hematology Unit, Necker Enfants Malades Hospital, 75015 Paris, France
[34]Howard Hughes Medical Institute, New York, NY 10065

CORRESPONDENCE
Stéphanie Boisson-Dupuis:
stbo603@rockefeller.edu

Abbreviations used: Ab, antibody; AD, autosomal dominant; AR, autosomal recessive; BCG, bacille Calmette–Guérin; CMC, chronic mucocutaneous candidiasis; EBV–B cell, EBV-transformed B cell; EMSA, electrophoretic mobility shift assay; GAF, gamma-activating factor; GAS, gamma-activated sequence; HIES, hyper-IgE syndrome; HVS–T cell, herpesvirus *Saimiri*–transformed T cell; ISRE, interferon-stimulated response element; LIF, leukemia inhibitory factor; MOI, multiplicity of infection; NGS, next-generation sequencing; RT-qPCR, RT–quantitative real-time PCR; SV40-fibroblast, simian virus 40–immortalized fibroblast; TAE, T cell activation and expansion; VSV, vesicular stomatitis virus; VZV, varicella zoster virus; WES, whole-exome sequencing.

The Rockefeller University Press $30.00
J. Exp. Med. 2015 Vol. 212 No. 10 1641–1662
www.jem.org/cgi/doi/10.1084/jem.20140280

Autosomal recessive, complete TYK2 deficiency was previously described in a patient (P1) with intracellular bacterial and viral infections and features of hyper-IgE syndrome (HIES), including atopic dermatitis, high serum IgE levels, and staphylococcal abscesses. We identified seven other TYK2-deficient patients from five families and four different ethnic groups. These patients were homozygous for one of five null mutations, different from that seen in P1. They displayed mycobacterial and/or viral infections, but no HIES. All eight TYK2-deficient patients displayed impaired but not abolished cellular responses to (a) IL-12 and IFN-α/β, accounting for mycobacterial and viral infections, respectively; (b) IL-23, with normal proportions of circulating IL-17$^+$ T cells, accounting for their apparent lack of mucocutaneous candidiasis; and (c) IL-10, with no overt clinical consequences, including a lack of inflammatory bowel disease. Cellular responses to IL-21, IL-27, IFN-γ, IL-28/29 (IFN-λ), and leukemia inhibitory factor (LIF) were normal. The leukocytes and fibroblasts of all seven newly identified TYK2-deficient patients, unlike those of P1, responded normally to IL-6, possibly accounting for the lack of HIES in these patients. The expression of exogenous wild-type *TYK2* or the silencing of endogenous *TYK2* did not rescue IL-6 hyporesponsiveness, suggesting that this phenotype was not a consequence of the *TYK2* genotype. The core clinical phenotype of TYK2 deficiency is mycobacterial and/or viral infections, caused by impaired responses to IL-12 and IFN-α/β. Moreover, impaired IL-6 responses and HIES do not appear to be intrinsic features of TYK2 deficiency in humans.

The first TYK2-deficient patient (P1) to be identified was reported in 2006 (Minegishi et al., 2006; Casanova et al., 2012). This patient was Japanese and displayed the triad of signs characteristic of hyper-IgE syndrome (HIES): atopic dermatitis, high circulating IgE levels, and recurrent cutaneous staphylococcal infections (Minegishi, 2009; Heimall et al., 2010; Chandesris et al., 2012; Sowerwine et al., 2012). He also suffered from intracellular bacterial infections, including lymphadenitis caused by live bacille Calmette–Guérin (BCG) vaccine, an attenuated strain of *Mycobacterium bovis*, and recurrent gastroenteritis caused by nontyphi *Salmonella*. P1 also developed viral infections, including parainfluenza virus (PIV) pneumonia, chronic skin *Molluscum contagiosum* infections, and recurrent oral HSV infections. The impaired IL-12 and IFN-α/β signaling in this patient accounted for intracellular bacterial and viral diseases. Impaired IL-6 and IL-10 responses were also documented, paving the way for the identification of autosomal dominant (AD) signal transducer and activator of transcription 3 (STAT3) deficiency in patients with full-blown HIES, including developmental features (Minegishi et al., 2007). Intracellular bacterial and viral infections are not generally observed in patients with AD-HIES (Minegishi, 2009; Chandesris et al., 2012; Sowerwine et al., 2012). The subsequent discovery of patients with IL-10, IL-10R1, or IL-10R2 deficiency and early-onset colitis but not HIES (Glocker et al., 2009, 2010) suggested that impaired responses to IL-6, but not IL-10, accounted for at least some features of the characteristic triad of signs seen in HIES patients with *TYK2* or *STAT3* mutations. The responses to other cytokines, including other members of the IL-6, IL-10, IL-12, and IFN-α/β cytokine families, had not previously been reported for this TYK2-deficient patient (Minegishi et al., 2006).

We report here the identification and immunological investigation of seven other TYK2-deficient patients from five unrelated families originating from Turkey, Morocco, Iran, and Argentina, whose clinical features were (Casanova et al., 2012; Kilic et al., 2012) or will be (unpublished data) described in detail elsewhere (also see Case reports in Materials and methods), which we compare with the Japanese patient (Fig. 1). In brief, a 23-yr-old Turkish patient (P2) suffered from intracellular bacterial infections, including BCG disease and *Brucella* meningitis, and recurrent cutaneous infections caused by varicella zoster virus (VZV; Kilic et al., 2012). A genome-wide linkage study identified TYK2 deficiency (Grant et al., 2011; Kilic et al., 2012). A 15-yr-old girl from Morocco (P3) died from disseminated tuberculosis, and her younger brother (P4) suffered from meningitis of unknown origin. A 5-yr-old boy from Iran (P5) developed BCG disease, and his younger sister suffered from BCG disease and cutaneous viral infections (P6). A 9-yr-old girl from Iran suffered from miliary tuberculosis (P7). An 11-yr-old boy from Argentina suffered from disseminated HSV disease (P8). Whole-exome sequencing (WES) and targeted next-generation sequencing (NGS) led to the identification of inherited TYK2 deficiency in these patients. Surprisingly, unlike P1, none of these seven newly identified TYK2-deficient patients displayed any of the features of HIES. In particular, they did not display atopy, high serum IgE concentration, or staphylococcal disease. We thus compared the cellular responses to a broad range of cytokines from the IL-12, IFN-α/β, IL-10, and IL-6 families in these patients. By delineating the public and private immunological phenotypes of the eight TYK2-deficient patients, we aimed to decipher the molecular and cellular basis of their public and private clinical phenotypes.

RESULTS

Identification of inherited TYK2 deficiency

We investigated the previously reported Japanese TYK2-deficient patient (P1; Minegishi et al., 2006). He carries a homozygous 4-bp deletion in exon 4 (Fig. 1, A–C). We also investigated seven patients (P2–P8) from five unrelated families from four different countries (Turkey, Morocco, Iran, and

*M.J. Ciancanelli, S. Okada, X.-F. Kong, and N. Ramírez-Alejo contributed equally to this paper.

**S.S. Kilic, J. El Baghdadi, S. Nonoyama, S.A. Mahdaviani, F. Ailal, A. Bousfiha, D. Mansouri, and E. Nievas contributed equally to this paper.

***L. Hammarstrom, A. Puel, S. Al-Muhsen, L. Abel, D. Chaussabel, S.D. Rosenzweig, Y. Minegishi, S.G. Tangye, and J. Bustamante contributed equally to this paper.

****J.-L. Casanova and S. Boisson-Dupuis contributed equally to this paper.

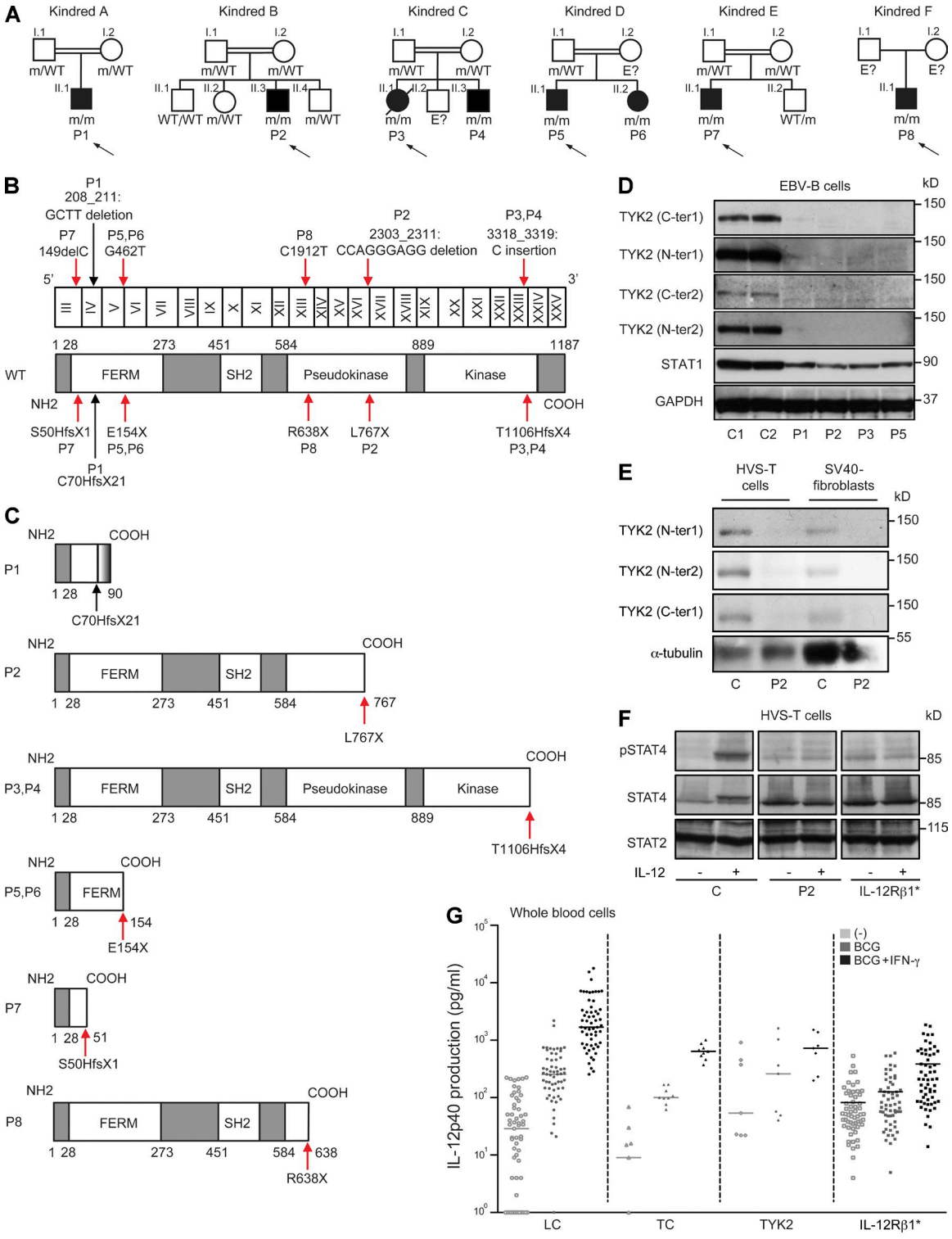

Figure 1. Familial segregation and expression of TYK2 in patients' cells. (A) Pedigrees of the TYK2-deficient families. Each generation is designated by a Roman numeral (I–II) and each individual by an Arabic numeral. The double lines connecting the parents indicate consanguinity. The probands (P1, P2, P3, P5, P7, and P8) in the six families are indicated by an arrow. Solid shapes indicate disease status. Individuals whose genetic status could not be determined are indicated by "E?", and "m" indicates a mutated allele. (B) Schematic representations of the *TYK2* gene with its 23 coding exons and of the TYK2 protein with its various domains (FERM, SH2, pseudokinase, and kinase). The exons are numbered with Roman numerals (III–XXV). The positions of the *TYK2* mutation previously reported for P1 and of the resulting premature STOP codon are indicated by black arrows. The positions of the mutations for P2–P8 and their premature STOP codons are indicated by red arrows. (C) The predicted proteins for P1, P2, P3, P4, P5, P6, P7, and P8 are represented.

Argentina) who suffered from mycobacterial and/or viral diseases (Table 1; Kilic et al., 2012; unpublished data). We identified homozygous mutations in *TYK2* by linkage analysis and Sanger sequencing (P2), WES (P3 to P7), or targeted NGS (P8). There is a 9-bp deletion in exon 16, *c.2303_2311del*, in P2 from kindred B (Fig. 1, A–C; Grant et al., 2011). In P3 and P4, from kindred C, there is a frameshift insertion of 1 bp in exon 23, *c.3318_3319insC* (Fig. 1, A–C). A nucleotide substitution in exon 5 (*c.462G>T*) in P5 and P6, from kindred D, leads to the creation of a premature stop codon at amino acid position 154 (E154X). A frameshift deletion of 1 bp at position 149 in exon 3 in P7 (*c.149delC*), from kindred E, leads to the creation of a premature stop codon at position 50 in the protein (S50HfsX1). A nucleotide substitution (*c.1912 C>T*) at position 1912 in exon 13 in P8, from kindred F, creates a premature stop codon at position 638 (R638X; Fig. 1, A–C). In all kindreds, clinical disease was observed in all of the homozygotes, and only in homozygotes. These five novel *TYK2* mutations, like that of P1, are predicted to result in a premature stop codon. They are also private, as they are absent from our in-house WES database and all public databases (including NCBI, Ensembl, 1,000 genomes, and ExAc). There are no homozygous individuals for stop mutations in any database and only 84 heterozygous individuals. Thus, the seven patients from five kindreds reported here probably had autosomal recessive (AR) TYK2 deficiency (Fig. 1, A–C).

TYK2 is not expressed in the patients' cells

Unlike P1, these seven patients displayed only intracellular bacterial and/or viral infections, with no features of HIES (Table 1; Kilic et al., 2012; unpublished data). We therefore characterized and compared TYK2 expression and function in all patients. The 9-bp deletion of P2 results in a premature stop codon at position 767 of the 1,187–amino acid TYK2 protein (Fig. 1, B and C). In P3 and P4, the frameshift generates a premature stop codon at amino acid position 1110. The nonsense mutations in P1, P5 and P6, and P8 are located upstream from P2, at positions 90, 154, and 638, respectively. The frameshift in P7 leads to an even earlier stop codon, at position 50. We investigated *TYK2* expression by examining the nature and amounts of mRNA in EBV-transformed B cell (EBV–B cell) lines from P1, P2, and P3. We used specific primers distinguishing between full-length and shorter transcripts to search for potential splice variants. No abnormal splicing was detected. We detected only normal-sized transcripts containing the deletion or the insertion for P2 and P3, respectively (not depicted), and smaller amounts of *TYK2* mRNA by quantitative PCR in P2 (not depicted). We then performed Western blotting with EBV–B cells from P1, P2, P3, P5, P7, and P8 and herpesvirus *Saimiri*–transformed T cells (HVS–T cells) and simian virus 40–immortalized fibroblasts (SV40-fibroblasts) from P2. We used four antibodies (Abs) recognizing N- or C-terminal epitopes of TYK2. The 130-kD TYK2 protein, which was detectable in control cells, was undetectable in cells from all patients (Fig. 1, D and E; and see Fig. 4 A). These results suggest that the seven newly identified patients (P2–P8), like P1, display complete TYK2 deficiency, with no residual production of the WT protein.

The scaffolding role of TYK2 is abolished in the patients' cells

We assessed the impact of TYK2 deficiency by evaluating the expression of receptors with expression at least partly dependent on the scaffolding role of TYK2 (Velazquez et al., 1995; Ragimbeau et al., 2003). For example, TYK2 contributes to the expression of IFN-αR1 in human fibrosarcoma cells (Ragimbeau et al., 2003). The absence of TYK2 leads to impaired IFN-αR1 expression on the surface of P1 T cells (Minegishi et al., 2006). We investigated the expression of this receptor in EBV–B cells from healthy controls and TYK2-deficient patients by flow cytometry. As shown in Fig. 2 A, TYK2-deficient cells displayed low levels of IFN-αR1 surface expression, whereas IFN-αR2, IFN-γR1, and IFN-γR2, which are not known to bind TYK2, were normally expressed (not depicted). We also assessed the expression of IL-10R2 and IL-12Rβ1, which are constitutively associated with TYK2 (Ghoreschi et al., 2009; Casanova et al., 2012; Stark and Darnell, 2012). As expected, IL-10R2– and IL-12Rβ1–deficient cells did not express the corresponding receptors. However, levels of IL-10R2 and IL-12Rβ1 were significantly lower in TYK2-deficient cells than in control cells. We also found that the ectopic expression of WT TYK2 in these cells rescued the surface expression of IFN-αR1, IL-10R2, and IL-12Rβ1 (Fig. 2 A). All the functional assays and the cells used are summarized in Table S1. These results highlight the essential role of TYK2 in the expression of receptors for various cytokines, including IFN-α/β, IL-12, IL-23, IL-10, and IFN-λ. In addition to this scaffolding role, TYK2 also has catalytic activity (Velazquez et al., 1992, 1995; Rani et al., 1999; Sohn et al., 2013). For example, human TYK2 catalytic activity is required for cellular responses to IL-12 and IL-23 but

(D) Levels of TYK2 in the patients' EBV–B cells. Western blotting was performed with two Abs recognizing the N-terminal epitopes from TYK2 (N-ter1 and N-ter2) and two Abs recognizing the C-terminal epitopes (C-ter1 and C-ter2). Proteins were extracted from EBV–B cells from two healthy controls (C1 and C2) and from the *TYK2*-mutated patients (P1, P2, P3, and P5). (E) TYK2 levels in the patients' HVS–T cells and SV40-fibroblasts from a healthy control and P2. Western blotting was performed with two Abs recognizing two different N-terminal epitopes from TYK2 (N-ter1 and N-ter2) and another Ab recognizing C-terminal epitopes (C-ter1). (F) Western blot showing the detection of phospho-STAT4 (pSTAT4) and STAT4 in HVS–T cells from a healthy control (C), P2, and an IL-12Rβ1–deficient patient (IL-12Rβ1*), not stimulated (−) or stimulated for 30 min with 50 ng/ml IL-12 (+). The results in D–F are representative of at least two independent experiments. (G) Response to BCG alone (MOI = 20) and BCG and IFN-γ (5,000 IU/ml), in terms of IL-12p40 production, as assessed by ELISA on whole blood samples from healthy controls (local controls, LC; travel controls, TC), the TYK2-deficient patients (P2 twice, P3, P4, P5, P6, and P7; TYK2), and IL-12Rβ1–deficient patients (IL-12Rβ1*). Mean values for each set of conditions are indicated by solid lines.

Table 1. Clinical and cellular phenotypes of TYK2-deficient patients

Parameter	Patient								Mouse data
	P1	P2	P3	P4	P5	P6	P7	P8	
Sex	Male	Male	Female	Male	Male	Female	Female	Male	
Country	Japan	Turkey	Morocco	Morocco	Iran	Iran	Iran	Argentina	
Atopy/ Dermatitis	yes	no	no	no	no	no	no	no	
High IgE levels	yes	no	no	no	no	no	no	no	
S. aureus infections	yes	no	no	no	no	no	no	no	
Viral infections	HSV, PI3, MC	VZV	no	yes?	no	yes	no	HSV	
Intracellular bacterial infections	BCG-osis, *Salmonella*	BCG-osis, *Brucella*	*M. tuberculosis*	yes?	BCG-osis	BCG-itis	*M. tuberculosis*	no	
Fungal infections	*C. albicans*	no	no	no	no	no	no	no	
Homozygous mutation	C70HfsX21	L767X	T1106HfsX4	T1106HfsX4	E154X	E154X	S50HfsX1	R638X	
BCG vaccination	yes	yes	yes	yes	yes	yes	yes	yes	
Response to IL-12 and IL-23	impaired	impaired	impaired	impaired	impaired	impaired	impaired	impaired	impaired
Response to IFN-α	impaired	impaired	impaired	impaired	impaired	impaired	impaired	impaired	impaired
Response to IL-10	impaired	impaired	impaired	impaired	impaired	impaired	impaired	impaired	normal
Response to IL-6	impaired	normal	normal	normal	normal	normal	normal	normal	normal

not IFN-α or IL-10 (Sohn et al., 2013). We thus investigated the cellular responses to various cytokines, thereby determining the global impact of a lack of TYK2 scaffolding and catalytic activity in the patients' cells.

Impaired but not abolished response to IL-12 in TYK2-deficient leukocytes

We assessed the cellular responses to cytokines of the IL-12 family. Microarray analysis after 12 h of stimulation demonstrated that the response to IL-12 was impaired but not abolished in TYK2-deficient HVS–T cells (Fig. 2 B) from P2, although other, less sensitive methods suggested that the defect was complete (Fig. 1 F and not depicted). Likewise, whole blood from P2, P3, P4, P5, P6, and P7 displayed impaired but not abolished IFN-γ induction after stimulation with BCG plus IL-12 for 48 h (Fig. 2 C). This contrasts with findings for IL-12Rβ1–deficient patients, whose cells do not respond at all to BCG plus IL-12 (Altare et al., 1998, 2001; Fieschi et al., 2003; de Beaucoudrey et al., 2010), and with previous studies showing no detectable IFN-γ production by T cells from P1 after stimulation with IL-12 plus IL-18 (Minegishi et al., 2006; Ma et al., 2012). We identified the TYK2-deficient PBMCs partially responsive to BCG plus IL-12 in P1, P2, and P4 by assessing the intracellular IFN-γ production of T and NK cells by flow cytometry (Fig. 2, D and E; and Fig. S1). IFN-γ production by both T cells and NK cells from P1, P2, and P4 was impaired but not abolished. As a positive control, the patients' NK and T cells displayed normal IFN-γ induction in response to stimulation with PMA-ionomycin (Fig. S1 D and not depicted). Finally, T cells stimulated with IL-12 alone (Fig. S1 G) or IL-12 plus IL-18 (Fig. S1 F) or naive and memory CD4 T cells stimulated with beads conjugated to mAbs specific for CD2/CD3/CD28, with (Fig. S1 A) or without (Fig. S1 B and see Fig. 6 H) culture in Th1 conditions (including IL-12), displayed impaired but not abolished IFN-γ production. In addition, the induction of *Tbet* by IL-12 in naive CD4 T cells from TYK2-deficient patients was found to be impaired, with respect to that in healthy controls (Fig. S1 C). Thus, complete TYK2 deficiency resulted in impaired but not abolished responses to IL-12 in both T cells and NK cells in these patients. These data might explain both the occurrence of mycobacterial diseases in TYK2-deficient patients and the relatively favorable response of these diseases to antibiotic treatment.

Impaired response to IL-23 in TYK2-deficient leukocytes

Cellular responses to IL-27, another member of the IL-12 family, and to IFN-γ and IL-21 were normal (Figs. 1 G and 3, A, F, and G; Kotlarz et al., 2013, 2014; Tangye, 2015). IL-23 is a heterodimeric cytokine of this family that signals via IL-23R, IL-12Rβ1, JAK2, and TYK2 (Watford et al., 2004).

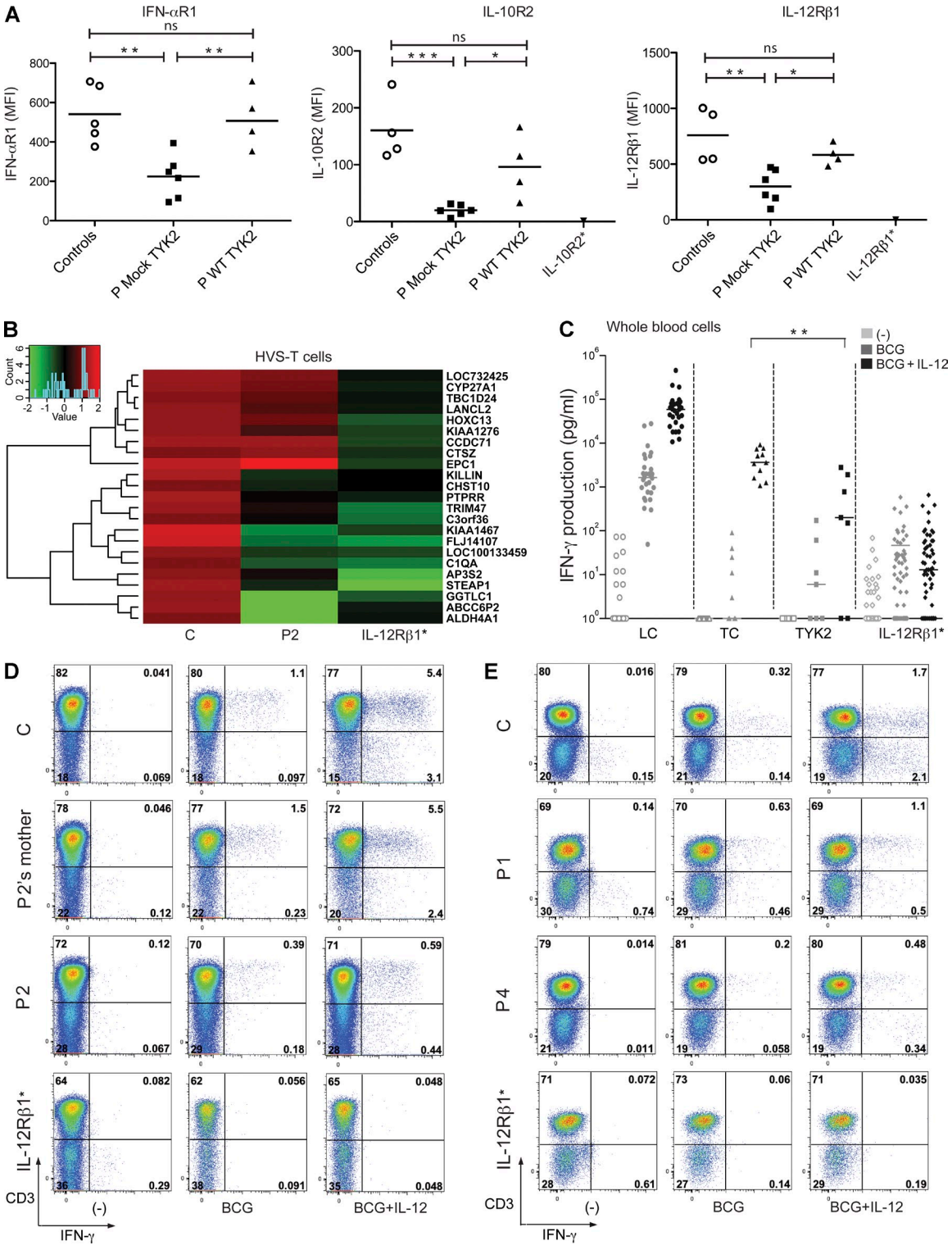

Figure 2. The IL-12 signaling pathway is impaired in TYK2-deficient patients. (A) Cell surface expression of IFN-αR1, IL-10R2, and IL-12Rβ1 was assessed in EBV-B cells from healthy controls, TYK2-deficient (P1, P2, P3, P5, P6, and P8) mock-transduced cells, TYK2-deficient (P1, P2, P3, and P5) WT TYK2-transduced cells, an IL-12Rβ1-deficient (IL-12Rβ1*) patient, and an IL-10R2-deficient patient (IL-10R2*) by flow cytometry. The results are expressed as mean fluorescence intensity (MFI). A p-value <0.05, <0.01, or <0.001 in two-tailed Student's *t* tests is indicated by *, **, or ***, respectively. ns, not significant. Mean values for each condition are indicated by solid lines. (B) Microarray analysis of HVS-T cell lines from three healthy controls, P2, and an IL-12Rβ1–deficient patient. Cells were stimulated for 12 h with 100 ng/ml IL-12. The difference between nonstimulated and stimulated cells is represented as fold change. (C) After 48 h, IFN-γ production was assessed by ELISA on supernatants from the whole blood of healthy donors (local controls, LC),

We investigated the response of HVS–T cells to IL-23 by microarray analyses, after stimulation for 12 h with IL-23, in three healthy controls, a TYK2-deficient patient (P2), and an IL-12Rβ1–deficient patient (Fig. 3 B). In contrast to the results obtained with less sensitive assays (not depicted), we detected impaired but not abolished responses in TYK2-deficient cells. In EBV–B cells (Fig. 3 C), the response was highly variable in healthy control cells, and a modest but reproducible phosphorylation of STAT3 was observed in response to IL-23 in some cells from P1, P2, P3, P5, P7, and P8 (Fig. 3 C). In the same assay, ectopic expression of WT TYK2 in cells from P1, P2, P3, and P5 restored their response to IL-23, in terms of STAT3 phosphorylation (Fig. 3 D). We also investigated the proportion of IL-17$^+$ T cells, which is low in some patients with IL-12Rβ1 deficiency, a subset of whom develop chronic mucocutaneous candidiasis (CMC), presumably because of impaired responses to IL-23 (de Beaucoudrey et al., 2008, 2010; Ouederni et al., 2014). Impaired IL-17 immunity underlies CMC, as IL-17F and IL-17RA mutations cause inherited forms of isolated CMC (Liu et al., 2011; Puel et al., 2011; van de Veerdonk et al., 2011; Boisson et al., 2013; Ling et al., 2015). Candidiasis was very mild in P1 (limited to a few episodes of mild oral candidiasis) and not observed at all in P2, P3, P4, P5, P6, P7, and P8. We found that P2, P4, and P8 had normal proportions of IL-17$^+$ T cells ex vivo (Fig. 3 E and not depicted). The percentage of IL-17A$^+$ memory CD4 T cells stimulated with CD2/3/28 beads also appeared to be normal (Fig. 3 J). We assessed the production of Th17 cytokines by naive CD4 T cells under Th17 culture conditions, in the presence of IL-23, in vitro. All three patients tested (P1, P2, and P4) displayed a profound impairment of IL-17A and IL-17F production (Fig. 3, H and I). Thus, the response to IL-23 is impaired but not abolished in TYK2-deficient patients. This results in an impairment of the generation of IL-17 T cells in vitro but not in vivo, probably accounting for the lack of overt CMC in the patients and implicating alternative pathways in the generation of human IL-17 T cells in the absence of TYK2-dependent IL-23 responses.

Impaired but not abolished early responses to IFN-α/β

We then investigated the molecular basis of viral diseases and the impact of TYK2 deficiency on responses to antiviral IFN-α/β. TYK2 acts downstream from the human IFN-α/β receptor (Velazquez et al., 1992; Stark et al., 1998). We investigated the cellular responses to IFN-α and IFN-β in EBV–B cells from P1, P2, P3, P5, P7, and P8 by Western blotting. After stimulation with IFN-α and IFN-β, we observed STAT1 phosphorylation in the cells of all patients, albeit at much lower levels than in a healthy control (Fig. 4, A and B). No STAT3 phosphorylation was detected in the patients' cells (Fig. 4, C and D). The phosphorylation of STAT3 but not STAT1 was detected in cells from a STAT1-deficient patient (Fig. 4, A and C; Dupuis et al., 2003). The phosphorylation of STAT1 and STAT3 was restored by the reexpression of WT TYK2 in EBV–B cells from P1, P2, P3, and P5 (Fig. 4 E). We then assessed the DNA-binding activity of IFN-α/β–induced gamma-activating factor (GAF) and interferon-stimulated gene factor 3 (ISGF3). P1, P2, and P3 showed impaired but not abolished responses to IFN-α/β in terms of GAF and ISGF3 DNA-binding activity (Fig. 4, F and G). The complexes formed consisted of STAT1/STAT1 dimers (GAF) and STAT1/STAT2/p48 trimers (ISGF3), as determined by supershift experiments (not depicted). The GAF-binding complexes in STAT1-deficient cells consisted of STAT3/STAT3 homodimers (Dupuis et al., 2003). We also investigated the response to IFN-α/β in SV40-fibroblasts and HVS–T cells from P2 (Fig. 4 H). Impaired IFN-α–induced ISGF3 DNA binding was detected in the SV40-fibroblasts (Fig. 4 H), whereas no response was detected in HVS–T cells (not depicted). These results suggest that IFN-α/β signaling is TYK2 dependent and that this dependence is stronger in HVS–T cells than in SV40-fibroblasts and EBV–B cells.

Impaired but not abolished late responses to IFN-α/β

We assessed late responses to IFN-α/β, such as the induction of target gene transcription and IFN-α–mediated protection during viral infection. After IFN-α/β stimulation for 2 and 6 h in EBV–B cells and SV40-fibroblasts, we showed by RT–quantitative real-time PCR (RT-qPCR) that cells from P1 and P2 responded normally in terms of the induction of *ISG15* and *MX1* transcription (Fig. 4 I and not depicted). However, the basal level of expression of these target genes was much lower in the patients than in controls. Moreover, we observed no STAT1-independent, STAT3-dependent induction of *SOCS3* transcription by IFN-α/β in EBV–B cells from P1 and P2 (not depicted; Dupuis et al., 2003). There was therefore a partially impaired response to IFN-α/β in TYK2-deficient EBV–B cells and SV40-fibroblasts. We then assessed vesicular stomatitis virus (VSV) replication in EBV–B cells from P1 and P2 and in HVS–T cells and SV40-fibroblasts from P2, with and without prior IFN-α treatment. In contrast to the results obtained for control cells, the prior treatment of EBV–B cells

patients' healthy relatives (travel controls, TC), TYK2-deficient patients P2 (tested twice), P3, P4, P5, P6, and P7 (TYK2), and IL-12Rβ1–deficient patients (IL-12Rβ1*), with and without stimulation with BCG alone (MOI = 20) or BCG and 20 ng/ml IL-12. As seen in the figure, transportation of the blood affects the response to BCG and BCG + IL-12. As the blood of all patients was transported before testing, the results are compared with those for travel controls. A p-value <0.01 for the two-tailed Student's *t* test for the comparison of travel controls and TYK2-deficient patients is indicated by **. Mean values for each set of conditions are indicated by solid lines. (D and E) Flow cytometry analysis showing intracellular IFN-γ production in PBMCs after stimulation in the absence (−) or presence of BCG (MOI = 20) or BCG and 100 ng/ml IL-12 for 48 h. An anti-CD3 Ab was used to identify CD3$^+$ T cells. (D) PBMCs from a healthy control (C), patient P2 (P2), his mother (P2's mother), and an IL-12Rβ1–deficient patient (IL-12Rβ1*). (E) PBMCs from a healthy control (C), patient P1 (P1), patient P4 (P4), and an IL-12Rβ1–deficient patient (IL-12Rβ1*).

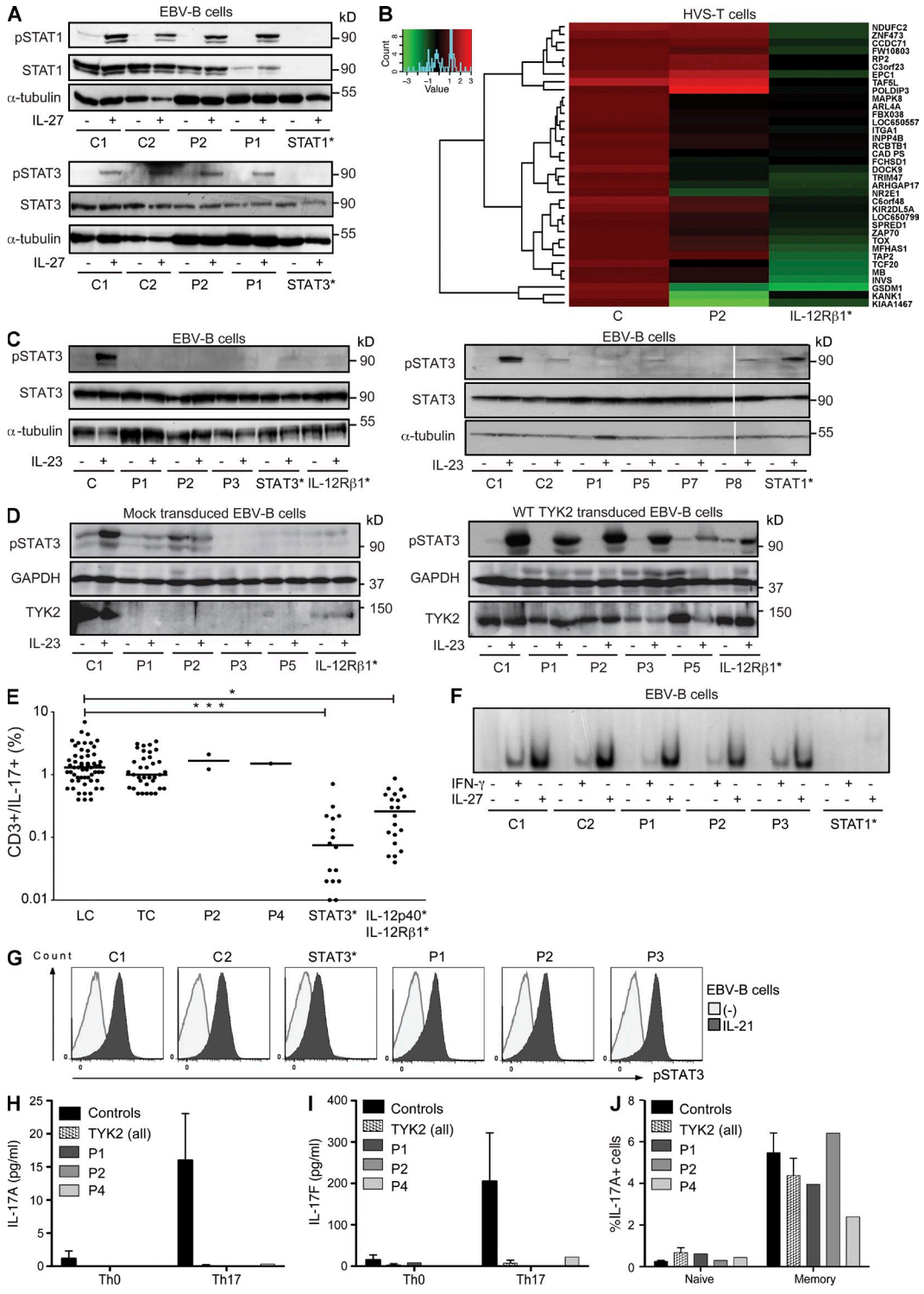

Figure 3. TYK2 deficiency impairs the response to IL-23 but not to IL-27 nor IFN-γ. (A) Western blot analysis of STAT1 (pSTAT1, top) and STAT3 (pSTAT3, bottom) phosphorylation in EBV-B cells from healthy controls (C1 and C2), TYK2-deficient patients (P1 and P2), a patient with complete STAT1 deficiency (STAT1*), and an AD-HIES patient with a heterozygous *STAT3* mutation (WT/T708N; STAT3*), after stimulation with 100 ng/ml IL-27 for 20 min. STAT1, STAT3, and α-tubulin levels were also assessed. The results shown are representative of at least two independent experiments. (B) Microarray analysis of HVS-T cell lines from three healthy controls, P2, and an IL-12Rβ1–deficient patient. Cells were stimulated for 12 h with 100 ng/ml IL-23. The difference between nonstimulated and stimulated cultures is shown as a fold change. (C) Western blot depicting phospho-STAT3 (pSTAT3) in EBV-B cells from a healthy control (C, C1, and C2), TYK2-deficient patients (P1, P2, P3, P5, P7, and P8), an AD-HIES patient carrying a heterozygous *STAT3* mutation (WT/T708N; STAT3*), an IL-12Rβ1–deficient patient (IL-12Rβ1*), and a STAT1-deficient patient (STAT1*), without (−) and with (+) stimulation for 30 min

and HVS–T cells from the patients with IFN-α did not lead to control of viral replication after 48 h of infection (Fig. 4, J and L). This is consistent with the previously reported poor control of HSV replication in B cells from P1 in the presence of exogenous IFN-α (Minegishi et al., 2006). IFN-α–treated fibroblasts from P2 were able to control viral infection normally in the first 6 h after infection. However, these cells displayed uncontrolled viral replication after 8 h (Fig. 4 K). Thus, unlike STAT1-deficient cells, TYK2-deficient SV40-fibroblasts can, at least partly, control viral infection upon treatment with IFN-α. These data are consistent with the viral phenotype of the TYK2-deficient patients, which is similar to that of patients with partial STAT1 deficiency (Chapgier et al., 2009; Kong et al., 2010) but less severe than that of patients with complete STAT1 deficiency (Dupuis et al., 2003; Chapgier et al., 2006; Vairo et al., 2011; Boisson-Dupuis et al., 2012).

Suboptimal response to IFN-λ

IFN-λs, including IFN-λ1 (IL-29), IFN-λ2 (IL-28A), and IFN-λ3 (IL-28B), belong to the IL-10 family and use a heterodimeric receptor composed of IFN-λR1 and IL-10R2 to signal via the JAK-STAT pathway and contribute to antiviral immunity (Kotenko et al., 2003). Upon IFN-λ receptor engagement, TYK2 is recruited to IL-10R2 (Kotenko and Langer, 2004), but the impact of TYK2 deficiency on this signaling pathway remains unclear. We investigated the cellular response to these cytokines by RT-qPCR, assessing the induction of transcription of a target gene (*IFIT1*) after 2 and 4 h of stimulation of EBV–B cells from a healthy control, P1, P2, a STAT1-deficient patient, and an IL-10R2–deficient patient (Glocker et al., 2009). IL-10R2–deficient patients have no overt viral phenotype, perhaps reflecting their death or bone marrow transplantation early in life, the redundancy of IL-10R2 for IFN-λ responses in humans, or the redundancy of IFN-λ immunity itself (Zhang et al., 2008; Glocker et al., 2009). Cells from the IL-10R2– and STAT1-deficient patients did not respond to IFN-λ stimulation (Fig. 5 A). The TYK2-deficient patients' cells responded normally to IFN-λ1 and IFN-λ3, although basal levels of *IFIT1* mRNA were extremely low (as in STAT1-deficient cells). These results suggest that the response to IFN-λ in vitro is not strictly dependent on TYK2 but that TYK2 may control the basal expression of IFN-λ target genes. It is unclear whether this cellular phenotype contributes to the viral disease of TYK2-deficient patients, as no genetic defect selectively affecting IFN-α/β or IFN-λ immunity has yet been identified (Jouanguy et al., 2007; Zhang et al., 2008).

Impaired but not abolished responses to IL-10

TYK2 is involved in cellular responses to IL-10 in human cells (Stahl et al., 1994; Ihle, 1995; Minegishi et al., 2006; Saito et al., 2011). The PBMCs of P1 displayed impaired induction of *SOCS3* transcription after IL-10 treatment. The inhibition of LPS-induced TNF production by IL-10 was also impaired in the macrophages of P1 (Minegishi et al., 2006). We studied EBV–B cells from healthy controls, P1, P2, and an IL-10R2–deficient patient. We investigated their response to IL-10 by electrophoretic mobility shift assay (EMSA) using a gamma-activated sequence (GAS) probe. No induction of DNA-binding activity was detected in the IL-10R2–deficient cells (Fig. 5 B). The observed DNA-binding complexes were shown by EMSA to be STAT1 homodimers, STAT1/STAT3 heterodimers, and STAT3 homodimers (not depicted). The TYK2-deficient patients had an impaired but not abolished response to IL-10, in terms of STAT3/STAT3 homodimers. The EBV–B cells of all TYK2-deficient patients also had low levels of STAT3 phosphorylation after IL-10 stimulation (Fig. 5 C). This impairment of STAT3 phosphorylation was rescued by the reintroduction of WT TYK2 into EBV–B cells from P1, P2, P3, and P5 (Fig. 5 D). SV40-fibroblasts from P2 also displayed impaired STAT3 phosphorylation after IL-10 stimulation (not depicted). The response to IL-10 was then analyzed by RT-qPCR, and P1 and P2 EBV–B cells were found to display equally strong impairments of the induction

with 100 ng/ml IL-23. α-Tubulin was used as a protein loading control. The results shown are representative of at least three independent experiments. After analysis by densitometry, a p-value <0.05 (0.0295) for the two-tailed Student's *t* test for the comparison of IL-23–stimulated controls and TYK2-deficient patients (TYK2) was found. White lines indicate that intervening lanes have been spliced out. (D) Western blot depicting phospho-STAT3 (pSTAT3) in mock-transduced (left) and TYK2-transduced (right) EBV–B cells from a healthy control and P1, P2, P3, and P5, without (−) and with (+) stimulation for 30 min with 100 ng/ml IL-23. (E) Flow cytometry analysis of blood from TYK2-deficient patients P2 and P4, healthy controls (local controls, LC; and travel controls, TC), STAT3-deficient patients (STAT3*), and IL-12p40– and IL-12Rβ1–deficient patients (IL-12p40* and IL-12Rβ1*), showing the percentage of $CD3^+$ T cells producing IL-17 ex vivo. A p-value <0.05 or <0.001 in two-tailed Student's *t* tests is indicated by * or ***, respectively. Mean values for each set of conditions are indicated by solid lines. (F) Responses to IFN-γ (10^5 IU/ml for 20 min) and IL-27 (100 ng/ml for 20 min) were evaluated by EMSA in EBV–B cells from the TYK2-deficient patients (P1, P2, and P3), two healthy controls (C1 and C2), and a STAT1-deficient patient (STAT1*), with a GAS probe. (G) Flow cytometry analysis to assess the phosphorylation of STAT3 (pSTAT3) in EBV–B cells from two healthy controls (C1 and C2), three TYK2-deficient patients (P1, P2, and P3), and an AD-HIES patient (STAT3*), left untreated (−) or treated with 100 ng/ml IL-21 for 15 min. Intracellular staining was performed with APC-conjugated anti–human pSTAT3 Ab. (H and I) Cytokine production by in vitro–differentiated naive $CD4^+$ T cells from control donors and TYK2-deficient patients (P1, P2, and P4). Naive ($CD45RA^+CCR7^+$) $CD4^+$ T cells were purified from the PBMCs of WT controls ($n = 6$) or TYK2-deficient patients P1, P2, and P4 and cultured for 5 d. Cells were cultured with TAE beads (anti-CD2/CD3/CD28) alone (Th0) or together with polarizing stimuli (TGFβ, IL-1β, IL-6, IL-21, IL-23, anti–IL-4, and anti–IFN-γ) to generate Th17 type cells. After 5 d, culture supernatants were assessed for the secretion of IL-17A or IL-17F with cytometric bead assays. (J) Naive and memory (defined as $CD45RA^-$) $CD4^+$ T cells from WT controls ($n = 5$) and TYK2-deficient patients ($n = 3$; P1, P2, and P4) were purified (>98% purity) by FACS and cultured with TAE beads (anti-CD2/CD3/CD28) for 5 d, and the $IL\text{-}17A^+$ cells were then assessed by flow cytometry. All error bars indicate SEM.

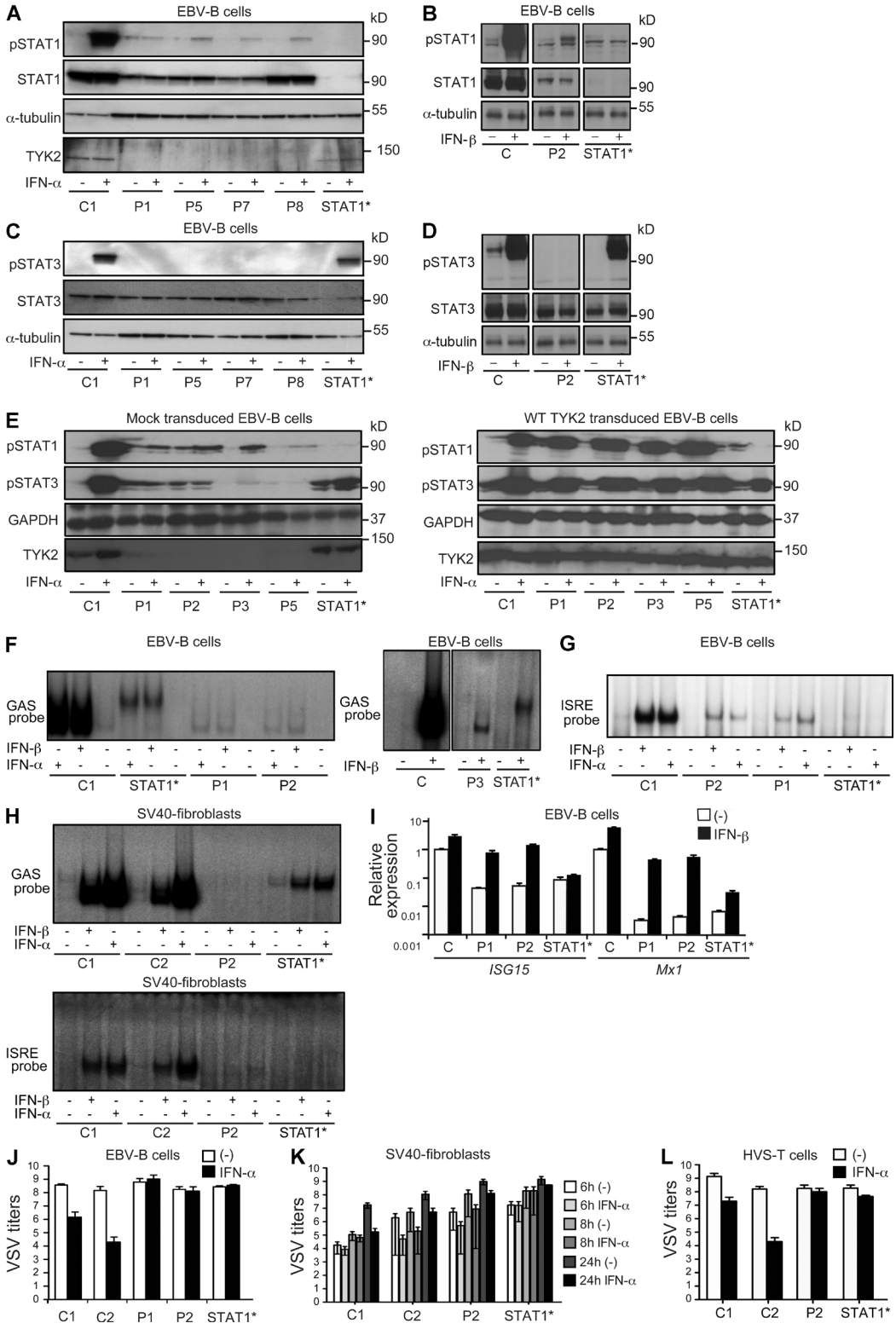

Figure 4. The response to type I IFNs in TYK2-deficient cells is impaired but not abolished. (A–D) Western blot of proteins extracted from EBV-B cells from a healthy control (C), TYK2-deficient patients (P1, P2, P5, P7, and P8), and a STAT1-deficient patient (STAT1*), with and without IFN-α (10^5 IU/ml) or IFN-β (3.2×10^4 IU/ml) stimulation for 30 min. (A and B) Abs against phosphorylated STAT1 (pSTAT1), STAT1, and tubulin were used. After analysis by densitometry, a p-value <0.01 (0.0018) for the two-tailed Student's *t* test for the comparison of IFN-α–pSTAT1 controls and TYK2-deficient patients (TYK2) was found. (C and D) Abs against phosphorylated STAT3 (pSTAT3), STAT3, and tubulin were used. After analysis by densitometry, a p-value <0.01 (0.0008) for the two-tailed Student's *t* test for the comparison of IFN-α–pSTAT3 controls and TYK2-deficient patients (TYK2) was found. (E) Western blot detecting

of *SOCS3* transcription (Fig. 5 E). We also assessed the suppression of LPS-induced TNF production by IL-10 in macrophages from a healthy control, P2 and his relatives, and a patient heterozygous for a *STAT3* mutation (Minegishi et al., 2006; de Beaucoudrey et al., 2008). P2's response to IL-10 was intermediate between those of healthy controls and the STAT3-mutated patient (Fig. 5 F). A severe intestinal phenotype is a characteristic clinical presentation of patients with IL-10, IL-10R1, and IL-10R2 deficiencies (Glocker et al., 2009, 2010, 2011). Residual cellular responses to IL-10 probably account for the lack of early-onset colitis in TYK2-deficient patients.

Divergent responses to IL-6 in cells from TYK2-deficient patients

Finally, we tested cellular responses to members of the IL-6 family. Responses to leukemia inhibitory factor (LIF) were normal in the only patient tested, P2 (Fig. 5, G and H). Impaired induction of *SOCS3* transcription in response to the IL-6 treatment of bulk PBMCs was previously documented for P1, together with an impairment of the induction of IgM secretion by the patient's B cells after the addition of IL-6 during EBV infection (Minegishi et al., 2006). Transduction of the IL-6 signal requires the binding of this cytokine to its receptor, IL-6R, the resulting complex then binding to a gp130 homodimer (Taga et al., 1989). This activates JAK1, JAK2, and TYK2, leading to STAT3-mediated signaling (Ihle and Kerr, 1995; Leonard and O'Shea, 1998). We thus assessed STAT3 phosphorylation upon IL-6 stimulation in EBV–B cells from healthy controls and TYK2-deficient patients (P1, P2, P3, P5, P7, and P8). Surprisingly, the responses of cells from P2, P3, P5, P7, and P8 were normal, at odds with the results for P1 (Fig. 6, A and B). We confirmed the hyporesponsiveness of P1 to IL-6 in an independent EBV–B cell line (not depicted). This phenotype was also confirmed by EMSA with a GAS probe (Fig. 6 C). In P1, we detected only a very small number of DNA-binding complexes, consisting of STAT3 homodimers, STAT1 homodimers, and STAT1/STAT3 heterodimers (Fig. 6 C and not depicted). Moreover, no binding complexes could be detected by EMSA-ELISA in P1 (not depicted). Finally, there was no induction of *SOCS3* transcription by hyper–IL-6 stimulation (a fusion of IL-6 and soluble IL-6R) in P1 cells, as assessed by quantitative PCR (not depicted; Fischer et al., 1997). These data confirmed the previously reported hyporesponsiveness to IL-6 of B cells from P1 (Minegishi et al., 2006) and also, surprisingly, showed that the EBV–B cells of all other TYK2-deficient patients tested responded normally to IL-6. Accordingly, primary fibroblasts from P2 phosphorylated STAT3 normally in response to IL-6, unlike P1 fibroblasts, which displayed an impaired response (Fig. 6 D). Fibroblasts from the other TYK2-deficient patients (P3–P8) were not available. Collectively, these results suggest that TYK2 was dispensable for adequate IL-6 signaling in all the TYK2-deficient patients tested other than P1.

Impaired responses to IL-6 in P1 cells are TYK2 independent

We investigated whether the homozygous *TYK2* mutation of P1 could be responsible for IL-6 hyporesponsiveness in two ways. First, we investigated whether WT TYK2 was required for IL-6 responses in P1, bearing in mind that it was not required in the other patients. Second, we assessed the remote but finite possibility that an abnormal and undetected product from the *TYK2* locus, other than the full-length *TYK2*, which is not expressed in P1, might interfere with IL-6 signaling in P1. We thus tested whether restoring WT *TYK2* expression in EBV–B cells from P1 by retroviral transduction could restore the response to IL-6. We found no clear difference in the level of STAT3 phosphorylation after IL-6 treatment in cells from P1 transduced with empty vector or TYK2 (Fig. 6 E), whereas STAT3 phosphorylation levels after IFN-β treatment were greater in TYK2-transduced cells than in mock-transduced cells. These data indicate that the hyporesponsiveness to IL-6 of P1 did not result from a lack of TYK2. We then did the reverse experiment, silencing the *TYK2* locus in EBV–B cells from a control and P1 using shRNAs (pools of three shRNA sequences targeting both the 5′ and 3′ of *TYK2* mRNA). The resulting decrease in *TYK2* mRNA and protein levels in control EBV–B cells had no effect on their response to IL-6, in terms of STAT3 phosphorylation (Fig. 6 F). Furthermore, decreasing the level of *TYK2* mRNA in P1 did not rescue the cells' response to IL-6 (Fig. 6 F and not depicted). These findings suggest that no abnormal

pSTAT1 and pSTAT3 in mock-transduced (left) or TYK2-transduced (right) EBV–B cells from a healthy control and P1, P2, P3, and P5, without (−) and with (+) stimulation for 30 min with 10^5 IU/ml IFN-α. (F and G) EMSA performed on EBV–B cells from a healthy control (C1), three TYK2-deficient patients (P1, P2, and P3), a patient with complete STAT1 deficiency (STAT1*), with (+) and without (−) stimulation with IFN-α (10^5 IU/ml) or IFN-β (3.2×10^4 IU/ml) for 30 min, with a GAS probe (F) or an ISRE probe (G). (H) EMSA performed on SV40-fibroblasts from healthy controls (C1 and C2), the TYK2-deficient patient P2 (P2), and a patient with complete STAT1 deficiency (STAT1*), with (+) and without (−) stimulation with 10^5 IU/ml IFN-α or 3.2×10^4 IU/ml IFN-β for 30 min, probed for GAS (top) and ISRE (bottom). (I) Induction of *ISG15* (left) and *MX1* (right) relative to *GUS*, as assessed by RT-qPCR on mRNA extracted from EBV–B cells from three healthy controls (mean C), TYK2-deficient patients (P1 and P2), and a patient with complete STAT1 deficiency (STAT1*), without (−) or with stimulation for 6 h with 3.2×10^4 IU/ml IFN-β. (J) EBV–B cells from two healthy controls (C1 and C2), two TYK2-deficient patients (P1 and P2), and a patient with complete STAT1 deficiency (STAT1*) were left untreated (−) or were treated with 10^5 IU/ml IFN-α 18 h before infection with VSV (MOI = 1). Viral load was determined at 48 h and is represented as $\log_{10}$TCID50/ml. (K) SV40-fibroblasts from two healthy controls (C1 and C2), TYK2-deficient patient P2 (P2), and a STAT1-deficient (STAT1*) patient were or were not (−) treated with 10^5 IU/ml IFN-α 18 h before infection with VSV (MOI = 10) for 6, 8, or 24 h. Viral load was determined at these three time points. (L) HVS-T cells from two healthy controls (C1 and C2), the TYK2-deficient patient P2 (P2), and a STAT1-deficient (STAT1*) patient were or were not (−) treated with 10^5 IU/ml IFN-α for 18 h before infection with VSV (MOI = 0.01). Viral load was determined at 48 h. All the results shown are representative of at least three independent experiments. All error bars indicate SEM.

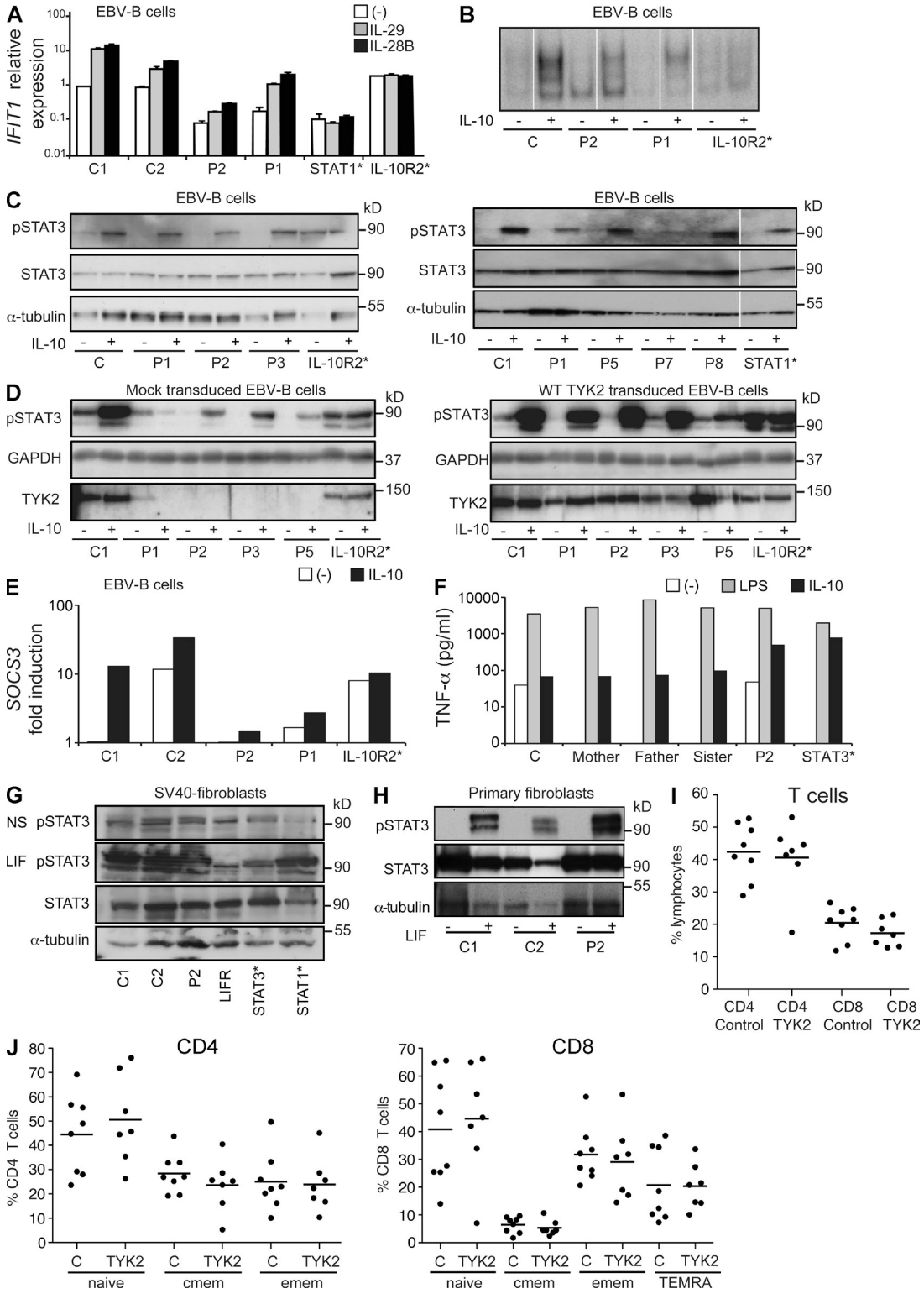

Figure 5. TYK2-deficient cells display an impaired response to IL-10 family cytokines. (A) The induction of *IFIT1* transcription was analyzed by RT-qPCR after the treatment for 2 h with 20 ng/ml IL-29 or IL-28B of EBV-B cells from two healthy controls (C1 and C2), two TYK2-deficient patients (P1 and P2), a patient with complete STAT1 deficiency (STAT1*), and an IL-10R2–deficient patient (IL-10R2*). Results are normalized with respect to *GUS* levels. Error bars indicate SEM. (B) EMSA was performed with a GAS probe and EBV-B cells from a healthy control (C), TYK2-deficient patients (P1 and P2), and an IL-10R2–deficient patient (IL-10R2*), with (+) and without (−) stimulation with 50 ng/ml IL-10 for 20 min. (C) Western blot of EBV-B cells from a healthy control (C), TYK2-deficient patients (P1, P2, P3, P5, P7, and P8), and an IL-10R2–deficient patient (IL-10R2*) after treatment with 50 ng/ml

product of the *TYK2* locus, specific to P1, was blocking the IL-6 responsive pathway. Thus, IL-6 signaling can be considered TYK2 independent in humans, as already shown in mice (Karaghiosoff et al., 2000; Shimoda et al., 2000), and the impaired response to IL-6 in P1 may be considered independent of the *TYK2* mutation in this patient. These findings also raise the intriguing question as to why the cells of P1 have an impaired response to IL-6. WES detected no mutation of any of the known components of the IL-6–responsive pathway (Itan et al., 2013, 2014), and protein levels for these components (JAK1, JAK2, gp130, and IL-6Rα) were identical to those in other TYK2-deficient patients (Fig. 6 G), suggesting that the patient may carry a variant of another, as yet unknown, component of this pathway.

DISCUSSION

We identified a Turkish patient (P2), whose clinical features have been reported elsewhere (Kilic et al., 2012), two Moroccan siblings (P3 and P4), three Iranian patients from two unrelated families (P5, P6, and P7), and an Argentinian patient (P8) with TYK2 deficiency and intracellular bacterial and viral infections but no HIES. The first TYK2-deficient patient to be described was Japanese and had HIES as the main clinical feature, associated with numerous intracellular infections (Minegishi et al., 2006). We characterized and compared the patients' cellular responses to multiple cytokines (a) to define the contribution of human TYK2 to the corresponding signaling pathways and (b) to determine the molecular and cellular basis of the private (HIES in P1 only) and public (intracellular bacterial and viral infections in all eight patients) clinical phenotypes of the patients. In the conditions tested, TYK2 was found to play a nonredundant role in signal transduction by five cytokine receptors, stimulated by IL-12, IL-23, IFN-α/β, IL-10, and IFN-λ. However, the defects are not complete, as residual TYK2-independent responses were observed upon treatment with these cytokines, implying that other molecules, such as other JAK kinases, can partially compensate for TYK2 deficiency. In contrast, TYK2 is apparently redundant for signal transduction downstream from receptors stimulated by IFN-γ, IL-27, IL-21, and LIF. These ex vivo and in vitro data suggest that TYK2 is redundant for these pathways in vivo. However, the pathways found to be TYK2 dependent in vitro may be affected to a greater or lesser extent in vivo.

Impaired responses to some of these cytokines may account for most of the clinical phenotypes of TYK2-deficient patients. Their susceptibility to intracellular bacteria, including *Mycobacterium*, *Salmonella*, and *Brucella*, is probably accounted for by the documented defects in IL-12–dependent IFN-γ immunity (Casanova and Abel, 2002, 2013; Rosenzweig and Holland, 2011; Casanova et al., 2013, 2014; Bustamante et al., 2014; Boisson-Dupuis et al., 2015). *Tyk2*$^{-/-}$ mice also display impaired responses to IL-12, with low levels of IFN-γ production (Karaghiosoff et al., 2000; Shimoda et al., 2000, 2002; Shaw et al., 2003; Tokumasa et al., 2007; Ishizaki et al., 2011), and susceptibility to intracellular pathogens, such as *Toxoplasma gondii* (Ortmann et al., 2001; Yap et al., 2001; Shaw et al., 2003; Strobl et al., 2011). Previous studies have suggested that human TYK2 is absolutely required for IL-12 responses (Minegishi et al., 2006; Ma et al., 2012). However, we have shown that TYK2-deficient T and NK cells retain a residual responsiveness to IL-12. This is consistent with the observation that infections with weakly virulent intracellular bacteria affecting these patients were curable with antibiotics and did not recur. However, one patient infected with virulent *Mycobacterium tuberculosis* died (P3), probably because IFN-γ production was insufficient. Overall, impaired IFN-γ production by TYK2-deficient T and NK cells in response to IL-12 stimulation probably accounts for the patients' susceptibility to intracellular bacteria. Four of the seven newly identified patients actually presented with a pure phenotype of MSMD (P4 and P5; Bustamante et al., 2014) or tuberculosis (P3 and P7; Casanova and Abel, 2002; Boisson-Dupuis et al., 2011), the other three resembling patients with partial forms of AR STAT1 deficiency (P2, P6, and P8; Chapgier et al., 2009; Kong et al., 2010). Interestingly, TYK2 deficiency is an additional cause of single-gene inborn errors of immunity that should be considered in cases of severe tuberculosis in children (Boisson-Dupuis et al., 2015).

The viral infections can probably be accounted for by defects of IFN-α/β and/or IFN-λ signaling (Kotenko et al., 2003; Pestka et al., 2004). TYK2 was identified as an essential

IL-10 for 15 min, probed with an Ab specific for phosphorylated STAT3 (pSTAT3). An Ab against tubulin was used as a loading control. After analysis by densitometry, a nonsignificant p-value for the two-tailed Student's *t* test for the comparison of IL-10–pSTAT3 controls and TYK2-deficient patients (TYK2) was found. (B and C) White lines indicate that intervening lanes were spliced out. (D) Western blot showing the detection of phospho-STAT3 (pSTAT3) in mock-transduced (left) or TYK2-transduced (right) EBV-B cells from a healthy control and P1, P2, P3, and P5, without (−) and with (+) stimulation for 30 min with 50 ng/ml IL-10. (E) *SOCS3* induction was analyzed by RT-qPCR after 6 h of treatment with 50 ng/ml IL-10, in EBV-B cells from two healthy controls (C1 and C2), TYK2-deficient patients (P1 and P2), and an IL-10R2–deficient (IL-10R2*) patient. Results are normalized with respect to *GUS*. The results shown in A–E are representative of at least two independent experiments. (F) Impaired response to IL-10 in the macrophages of P2. The inhibition of TNF production in response to LPS and IL-10 was assessed by ELISA in macrophages from a travel control (C), P2's relatives (mother, father, and sister), P2, and a patient with AD-HIES (STAT3*). (G and H) Western blots assessing the phosphorylation of STAT3 (pSTAT3) in healthy controls (C1 and C2), a TYK2-deficient patient (P2), an AD-HIES patient (STAT3*), and a patient with complete STAT1 deficiency (STAT1*), with (+) or without (−) LIF (100 ng/ml for 15 min). (G) In SV40-fibroblasts. (H) In primary fibroblasts. (I and J) Total CD4 and CD8 T cells (I) and naive (CCR7$^+$CD45RA$^+$), central memory (CCR7$^+$ CD45RA$^-$; cmem), effector memory (CCR7$^-$CD45RA$^-$; emem), and revertant effector memory (CCR7$^-$CD45RA$^+$) T cells in CD4$^+$ (J, left) and CD8$^+$ T cells (J, right) from healthy controls (C) and the TYK2-deficient patients P1, P2 (tested three times), P4 (tested twice), and P5 (TYK2). Mean values for each set of conditions are indicated by solid lines.

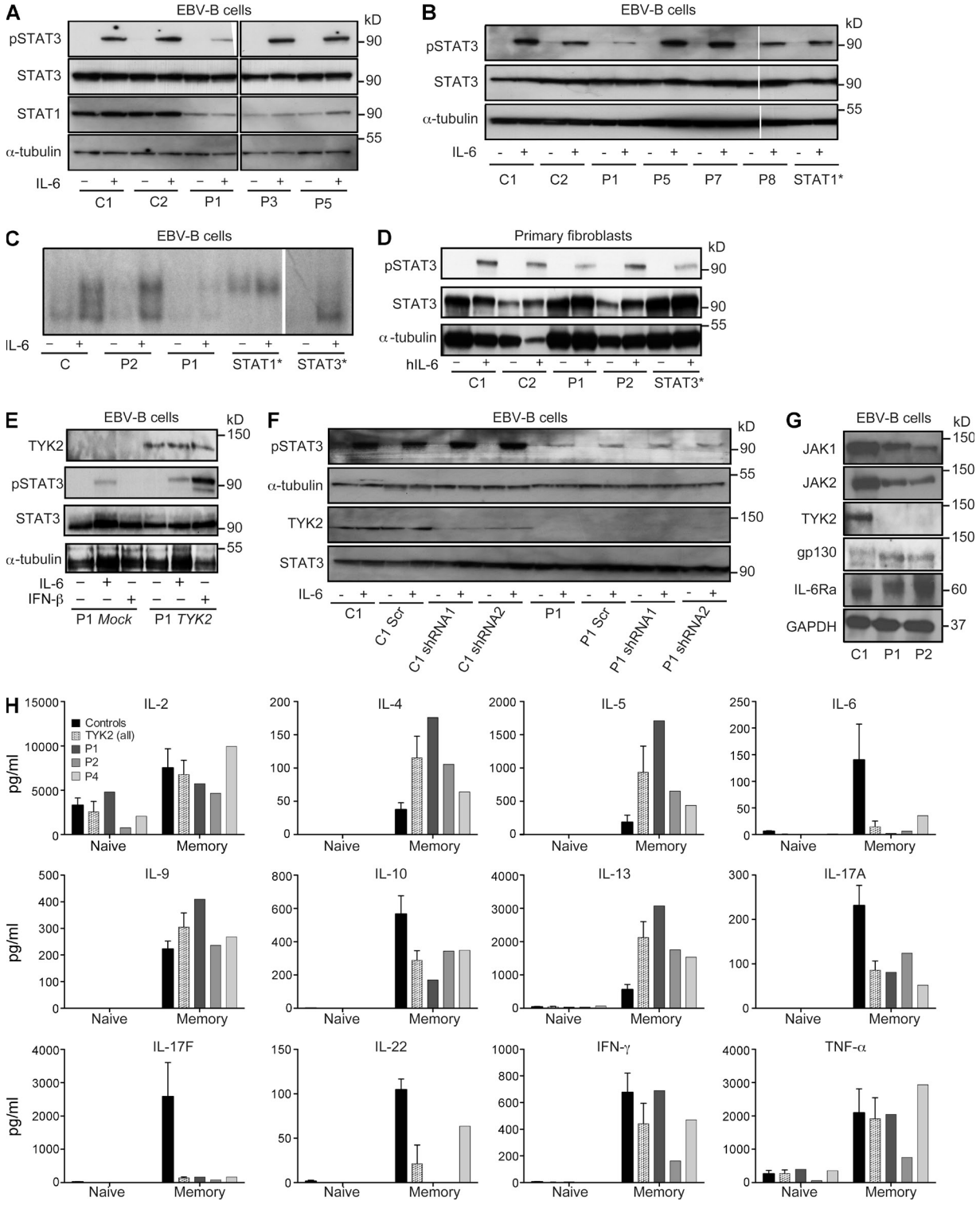

Figure 6. Divergent responses to IL-6 in the TYK2-deficient patients. (A and B) Western blot of EBV–B cells from a healthy control (C1 and C2), TYK2-deficient patients (P1, P3, P5, P7, and P8), and an AD-HIES patient heterozygous for a *STAT3* mutation (WT/S614G; STAT3*) after treatment with 50 ng/ml IL-6 for 20 min, probed with an Ab specific for phosphorylated STAT3 (pSTAT3). After analysis by densitometry, a p-value <0.05 (0.0332) for the two-tailed Student's *t* test for the comparison of IL-6–pSTAT3 controls and P1 was found. However, a nonsignificant result was obtained for the comparison of IL-6–pSTAT3 controls and other than P1 TYK2-deficient patients. (C) EMSA with a GAS probe on EBV–B cells from a healthy control (C), TYK2-deficient patients (P1 and P2), a STAT1-deficient patient (STAT1*), and a heterozygous AD-HIES patient (WT/S614G for *STAT3*; STAT3*), without (−) and with (+) stimulation with 50 ng/ml IL-6 for 20 min. (B and C) White lines indicate intervening lanes were spliced out. (D) Western blot of primary fibroblasts from two

component of the IFN-α/β-signaling pathway in a human fibrosarcoma cell line (Velazquez et al., 1992). However, *Tyk2*$^{-/-}$ mice display only a partial impairment of the response to IFN-α/β (Karaghiosoff et al., 2000; Shimoda et al., 2000; Prchal-Murphy et al., 2012). Nevertheless, these mice are susceptible to several viruses (Karaghiosoff et al., 2000; Strobl et al., 2011). The abolition of IFN-α/β signaling in P1 (Minegishi et al., 2006) was surprising, as this patient displayed few and mild viral infections. This contrasts with the various life-threatening viral infections of patients with complete STAT1 (Dupuis et al., 2003; Chapgier et al., 2006; Vairo et al., 2011; Boisson-Dupuis et al., 2012) or STAT2 (Hambleton et al., 2013) deficiency. Interestingly, three other TYK2-deficient patients displayed viral diseases of favorable outcome, and four did not display any viral illness. As a possible explanation, we showed that TYK2 plays a partly redundant role in IFN-α/β signaling. Although impaired IFN-λ signaling in TYK2-deficient patients may contribute to their viral phenotype, residual signaling may also explain the rarity and favorable outcome of viral infections in these patients. Impaired T cell memory is less likely to be involved, as no such defect was documented in TYK2-deficient patients, in contrast to *STAT3*-mutated HIES patients (Siegel et al., 2011; Ma et al., 2012; Ives et al., 2013). Overall, the viral infections seen in four of the eight TYK2-deficient patients can be accounted for by impaired responses to IFN-α/β and, perhaps, IFN-λ. Their mild features and the absence of viral infections in the other four patients probably result from residual responses to these IFNs.

A similar mechanism probably accounts for the lack of CMC in TYK2-deficient patients. CMC and impaired IL-17 T cell development occur in no more than 30% of IL-12Rβ1–deficient patients, although all display abrogated responses to IL-23 (de Beaucoudrey et al., 2008; Ma et al., 2008; Liu et al., 2011; Puel et al., 2011; Ouederni et al., 2014). Residual IL-23 responses in vivo in TYK2-deficient patients probably account for both the normal IL-17$^+$ T cell counts and lack of CMC. TYK2-deficient patients also have impaired IL-10 responses. It has recently been suggested that an impaired response to IL-10 contributes to the development of atopy in HIES patients (Saito et al., 2011). However, IL-10–, IL-10R1–, and IL-10R2–deficient patients do not seem to display HIES-like atopy (Glocker et al., 2009, 2010, 2011; Mao et al., 2012; Beşer et al., 2014). However, these patients died early in life or underwent hematopoietic stem cell transplantation, precluding accurate comparison. Moreover, P1 (who displays atopy) and P2, P3, P5, P7, and P8 (who do not display atopy) have equally impaired but not abolished responses to IL-10. This suggests that biological differences between P1 and the other seven patients, other than IL-10 responsiveness, are at work. Altogether, given that the response to the cytokines IFN-α, IL-12, IL-23, and IL-10 are equally impaired in all TYK2-deficient patients (including P1), defects in these responses are unlikely to be the cause of HIES in P1.

Studies of the pathogenesis of staphylococcal disease in *STAT3*-mutated HIES patients may help us to understand some of the features of HIES in P1. Defects in STAT3-mediated signaling play a key role in the development of HIES (Holland et al., 2007; Minegishi et al., 2007; Paulson et al., 2008; Minegishi, 2009), and STAT3 is essential for signal transduction for multiple cytokines, including IL-6. However, TYK2 deficiency in human fibrosarcoma cells does not affect the activation of STAT3 upon treatment with IL-6 (Guschin et al., 1995). In addition, all TYK2-deficient patients other than P1 (P2–P8) responded normally to IL-6. Impaired IL-6 signaling in P1 may therefore underlie HIES, or at least the staphylococcal infections in these patients. One child and two adults with autoantibodies against IL-6 have been reported to display staphylococcal diseases (Puel et al., 2008; Nanki et al., 2013). Moreover, IL-6–knockout mice are susceptible to systemic infections with several pyogenic bacteria (Dalrymple et al., 1996; van der Poll et al., 1997; van Enckevort et al., 2001; Cole et al., 2003; Diao and Kohanawa, 2005; Jones et al., 2006). IL-6–deficient mice have not yet been subjected to systemic challenge with *Staphylococcus aureus* but are vulnerable to *S. aureus* keratitis (Hume et al., 2006). The molecular basis of the intriguingly discrepant IL-6 responses of P1 and the seven other TYK2-deficient patients is unknown. In mice, IL-6 signaling is TYK2 independent (Karaghiosoff et al., 2000; Shimoda et al., 2000). The poor IL-6 responses seen in P1 but not in the other seven TYK2-deficient patients probably underlie at least the staphylococcal diseases, and perhaps other HIES phenotypes, of P1, although a role for other pathways (not studied here) cannot be ruled out. With hindsight, it is serendipitous that the discovery of IL-6 hyporesponsiveness in TYK2-deficient P1 with HIES led to the identification of *STAT3* mutations in patients with AD-HIES (Minegishi et al., 2007).

healthy controls (C1 and C2), two TYK2-deficient patients (P1 and P2), and a patient with AD-HIES (STAT3*), with (+) or without (−) hIL-6 (30 ng/ml for 30 min) stimulation, probed with an Ab specific for phosphorylated STAT3 (pSTAT3). (A, B, and D) An anti-tubulin Ab was used as a loading control. (E) Western blot of proteins extracted from EBV–B cells from the TYK2-deficient patient P1 stably transduced with mock (P1 *Mock*) or WT *TYK2* (P1 *TYK2*) retroviral particles. Cells were (+) or were not (−) stimulated with 50 ng/ml IL-6 and/or 3.2×10^4 IU/ml IFN-β for 15 min, as indicated. Abs against TYK2, phosphorylated STAT3 (pSTAT3), STAT3, and tubulin were used. (F) Western blot of proteins extracted from EBV–B cells from the TYK2-deficient patient P1 stably transduced with retroviral particles encoding the scramble shRNA (Scr) or shRNA specifically targeting TYK2 (shRNA1 or 2). Cells were (+) or were not (−) stimulated with 50 ng/ml IL-6 for 20 min. Abs against TYK2, phosphorylated STAT3 (pSTAT3), STAT3, and tubulin were used. All the results shown represent at least two independent experiments. (G) Western blot of EBV–B cells from a control (C) and from P1 and P2, assessing the expression of components of the IL-6 pathway: JAK1, JAK2, gp130, IL-6Ra, and TYK2. (H) Naive and memory (defined as CD45RA$^-$) CD4$^+$ T cells from WT controls ($n = 5$) and TYK2-deficient patients ($n = 3$; P1, P2, and P4) were purified (>98% purity) by FACS and cultured with TAE beads (anti-CD2/CD3/CD28) for 5 d, and the culture supernatants were then assessed for secretion of the cytokine indicated by cytometric bead assays or ELISA. Error bars indicate SEM.

MATERIALS AND METHODS

Case reports. The first patient investigated was a Japanese man (P1) with consanguineous parents. As described elsewhere (Minegishi et al., 2006), P1 has displayed atopic dermatitis since the age of 1 mo and recurrent bacterial and viral infections since the age of 1 yr. In particular, he developed BCGitis at the age of 22 mo, 6 mo after vaccination, and he has repeatedly suffered from skin abscesses caused by *S. aureus*, pneumonia (but without pneumatocele formation), otitis, and sinusitis. At the age of 15 yr, he was admitted to hospital with sepsis after severe nontyphi *Salmonella* enterocolitis. He has had to be hospitalized on several occasions for severe viral infections, including pneumonia caused by PIV3 and recurrent oral HSV infections associated with tonsillitis. Other viral infections have included *M. contagiosum*. P1 has also suffered from fungal infections, such as mild oral candidiasis caused by *Candida albicans*. Immunological explorations have repeatedly revealed hypereosinophilia (701–800/μl) and high serum IgE concentrations (1,430–2,100 IU/ml). This patient was diagnosed with AR-HIES on the basis of his NIH score of 48 points (Grimbacher et al., 1999). P1 is now 30 yr old and is regularly followed clinically in Japan. He is currently suffering from ocular sarcoidosis.

The second patient is a Turkish man (P2) born to consanguineous parents (first-degree cousins). A detailed clinical study relating to this patient has recently been published elsewhere (Kilic et al., 2012). In brief, this patient displayed disseminated BCG lymphadenitis at 21 mo of age and severe bacterial meningitis (with CFS cultures positive for *Brucella* spp.) at 8 yr of age, and at the age of 11 yr, he was diagnosed with shingles affecting the right maxillary branch of the trigeminal nerve. P2 is now 23 yr old and is followed in Turkey.

Two other patients, Moroccan siblings, a girl (P3) and a boy (P4), also born to consanguineous parents (first-degree cousins), were also identified. A detailed clinical study relating to these patients will be published elsewhere. In brief, both P3 and P4 were vaccinated with BCG at birth, with no adverse effects. P3 was hospitalized at the age of 13 yr with suspected abdominal tuberculosis. Despite antimycobacterial treatment, the abdominal complaints persisted, and P3 also suffered from ascitis and a psoas abscess that developed after a few months. *M. tuberculosis* was isolated from the abscess fluid culture, confirming the diagnosis of disseminated extrapulmonary tuberculosis. Treatment was restarted, but the patient was readmitted to hospital with bacterial meningitis and subsequently died, 15 mo after the initial onset of symptoms. P3's younger brother (P4) was hospitalized at the age of 8 mo for meningitis of unknown etiology. He suffered from recurrent otitis and urinary tract infections and presented asthma and eczema of the ear canal. His eosinophil levels were found to be high. P4 is now 15 yr old, has no treatment, and is followed in Morocco.

The fifth patient, P5, is a 5-yr-old boy born to consanguineous Iranian parents. He was vaccinated at birth with live BCG. At 2 and 4 mo of age, he developed right axillary lymphadenitis and multiple cervical lymphadenitis, respectively. Acid-fast bacilli were observed during an episode of lymphadenitis at the age of 2 yr. P5 was treated for 5 mo with antibiotics (isoniazid, rifampin, ethambutol, and pyrazinamide). At the age of 4.5 yr, he developed paravertebral and psoas abscesses with fistulization and pulmonary involvement. He was treated with isoniazid, rifampin, ethambutol, and streptomycin. Surgery was performed and antibiotic treatment continued (isoniazid, rifampin, ethambutol, streptomycin, ofloxacillin, and clarithromycin), together with IFN-γ. P5 is now 6 yr old and is followed in Iran. His younger sister (P6) is 2 yr old and was vaccinated with BCG at birth. She developed BCG lymphadenopathy, lasting for 1 mo, after vaccination. At the age of 1 yr, she was hospitalized for 1 wk for an unknown viral infection of the skin. She is now doing well without prophylaxis.

The seventh patient is a 9-yr-old girl from Iran born to consanguineous parents. She presented with a history of fever and productive cough that appeared 2 wk before she was referred to the hospital. She had also had close contact with a known case of tuberculosis (her grandfather). She had an uneventful history of vaccination (including BCG). She had an episode of pneumonia at 8 mo of age. At the age of 9 yr, spiral lung CT with contrast showed diffuse bilateral micronodular infiltrations associated with hilar and mediastinal adenopathies and cavitary consolidation in the right upper lobe. Abdominal CT showed left paraaortic adenopathies in the vicinity of the renal vein. No evidence of ascites was found. *M. tuberculosis* was identified on gastric washes by PCR and culture.

The eighth patient (P8) is an 11-yr-old boy from Argentina who was adopted at the age of 1 d. He was vaccinated with BCG, with no complications, at birth. At the age of 8 mo, he was clinically diagnosed with exanthema subitum. He successively suffered from herpes gingivostomatitis at 18 mo of age, aseptic meningitis (fever, vomiting, irritability, and altered mental state/reduced consciousness), and disseminated cutaneous herpetic lesions at 24 mo of age. He was treated with acyclovir for 10 d, with a good clinical response. At the age of almost 6 yr, he developed herpes gingivostomatitis and facial skin lesions, and, at the age of 10 yr, he was admitted with aseptic herpes meningitis and disseminated cutaneous herpetic lesions (HSV PCR: positive). He also has mild mental disability, and it has not been clearly established whether this disability is congenital or occurred after meningitis. The patient is now on acyclovir prophylaxis, which has helped deal with recurrences of oral/cutaneous herpes.

None of these newly identified patients (P2, P3, P4, P5, P6, P7, and P8) suffered from documented pyogenic infections, including staphylococcal diseases in particular, or from fungal infections, including mucocutaneous candidiasis in particular. Serum IgE levels have been determined on multiple occasions and have never been found to be high.The clinical information for all the patients is summarized in Table 1. Informed consent for participation in this study was obtained in accordance with local regulations, with approval from the Institutional Review Board (IRB). The experiments described here were performed in the United States of America, in accordance with local regulations and with the approval of the IRB of The Rockefeller University, New York.

Immunological studies: memory T cell compartment in the patients. In mice, several signaling pathways and cytokines, including IL-10 (Foulds et al., 2006), IL-21 (Elsaesser et al., 2009; Fröhlich et al., 2009; Yi et al., 2009), and IL-6 (Pellegrini et al., 2011), all of which signal principally via STAT3, contribute to the generation of $CD8^+$ T cell memory. In humans, a predisposition to chronic viral infections, such as VZV reactivation and EBV viremia, is observed in AD-HIES patients with *STAT3* mutations (Siegel et al., 2011). Recent studies have shown that these AD-HIES patients have fewer $CD4^+$ and $CD8^+$ central memory T cells than normal, potentially contributing to their inability to control these chronic viral infections (Siegel et al., 2011; Ives et al., 2013). The mucocutaneous viral infections observed in TYK2-deficient patients resemble the reactivation of chronic VZV and HSV infections. We therefore investigated whether TYK2-deficient patients also had abnormally small numbers of central memory T cells by assessing CCR7 and CD45RA expression in $CD4^+$ and $CD8^+$ T cells by flow cytometry. We observed that the TYK2-deficient patients P1, P2 (tested three times), P3, P4, and P5 had similar numbers of central memory ($CD4^+CCR7^+CD45RA^-$ and $CD8^+CCR7^+CD45RA^-$) T cells to healthy controls (Fig. 5, I and J), whereas AD-HIES patients generally have fewer such cells. Effector memory ($CD4^+CCR7^-CD45RA^-$, $CD8^+CCR7^-CD45RA^-$, and $CD8^+CCR7^-CD45RA^+$) T cell numbers were also similar in TYK2-deficient patients and healthy controls. Overall, our data suggest that the episodes of chronic viral infection reactivation observed in the TYK2-deficient patients cannot be accounted for by an impaired memory T cell compartment and that they instead probably result essentially from the impaired response to IFN-α/β.

Extraction of DNA and RNA, PCR, and sequencing. Human genomic DNA (gDNA) was isolated from blood, EBV-transformed lymphoblastoid cell lines (EBV–B cell lines), HVS–T cells, and SV40-transformed fibroblast cell lines (SV40-fibroblasts) by phenol/chloroform extraction, as previously described (Dupuis et al., 2003). Total RNA was extracted from the cells with TRIzol (Invitrogen), and RT was performed with Superscript II (Invitrogen), according to the kit manufacturer's instructions. PCR amplification was then performed with 50 ng DNA as the template and *Taq* DNA polymerase from Applied Biosystems and Invitrogen. Specific primers for amplifying *STAT1*

and *TYK2* from gDNA or cDNA were used and are available upon request. Amplified gDNA and cDNA PCR products were analyzed by electrophoresis in a 1% agarose gel and purified on Sephadex G-50 Superfine resin on filter plates (EMD Millipore). PCR products were sequenced by dideoxynucleotide termination, with the BigDye Terminator kit (Applied Biosystems). Purified PCR products were then sequenced on a 3700 apparatus (Applied Biosystems) and analyzed with GenalysWin 2.8 software.

WES. Massively parallel sequencing was performed on DNA extracted from EBV–B cells from P1, P2, and P3. In brief, the patients' DNA was sheared with a Covaris S2 Ultrasonicator (Covaris). An adapter-ligated library was prepared with the Paired-End Sample Prep kit V1 (Illumina). Exome capture was performed with the SureSelect Human All Exon kit (Agilent Technologies). Single-end sequencing was performed on a Genome Analyzer IIx (Illumina), generating 72-base reads. As described elsewhere (Byun et al., 2010), these sequences were aligned with the human genome reference sequence (hg18 build) using BWA aligner. Three open-source packages were used for downstream processing and variant calling (GATK, SAMtools, and Picard Tools). Substitution calls were made with GATK UnifiedGenotyper, whereas indel calls were made with GATK IndelGenotyperV2. All calls with a read coverage ≤4× and a phred-scaled quality of ≤30 were filtered out. All the variants were annotated with the SeattleSeq SNP annotation. Targeted NGS was performed as described elsewhere (Stoddard et al., 2014).

Cell culture and stimulations. EBV–B cell lines were cultured in RPMI (Invitrogen), and SV40-fibroblasts and 293T HEK cells were cultured in DMEM (Invitrogen) supplemented with 10% FBS (Invitrogen). *Saimiri* T cells were cultured in a 1:1 mixture (by volume) of RPMI and Panserin 401 (PAN-Biotech GmbH), supplemented with 10% FBS, 350 µg/ml glutamine, 100 µg/ml gentamycin, and 10 U/ml hIL-2 (Roche). PBMCs were isolated from blood by Ficoll-Hypaque density gradient centrifugation (GE Healthcare) and cultured at a density of 10^6 cells/ml in RPMI supplemented with 10% FBS. Stimulations were performed, at the doses stated and for the indicated times, with IL-12 (R&D Systems), BCG (donated by C. Nathan, Weill Cornell Medical College, New York, NY), IL-18 (R&D Systems), PMA/ionomycin (Sigma-Aldrich), IL-2 (BD), IL-23 (R&D Systems), IFN-γ (Imukin; Boehringer Ingelheim), IL-27 (R&D Systems), IFNα-2b (Intron A; Schering Plough), IFNβ-1b (PeproTech), LPS (Sigma-Aldrich), IL-21 (R&D Systems), IL-29 (R&D Systems), IL-28B (R&D Systems), IL-10 (R&D Systems), IL-6 (R&D Systems), hyper–IL-6 (hIL-6; donated by S. Rose-John), and LIF (EMD Millipore). hIL-6 was prepared as described elsewhere (Fischer et al., 1997).

Plasmids and retroviral transduction of EBV–B cells and SV40-fibroblasts. A retroviral vector expressing WT *TYK2* was generated by inserting the *TYK2* sequence from pCMV6-TYK2-GFP (OriGene) into the pMSCVpuro retrovirus (Takara Bio Inc.). Retroviral vectors were packaged with the Pantropic Expression System (BD). EBV–B cells were transduced by spinoculation. Stable cell lines were established by selection on 0.65 µg/ml puromycin, beginning 72 h after transduction. SV40-fibroblasts were transiently transduced by infection with the retroviruses in the presence of 4 µg/ml Polybrene. Cells were collected 48 h after infection.

Western blotting. Total protein was extracted from the cells with a lysis buffer containing 1% NP-40, 20 mM Tris-HCl, pH 7.4, 140 mM NaCl, 2 mM EDTA, and 50 mM NaF, supplemented with 100 mM orthovanadate, 200 mM PMSF, 1% aprotinin, 1 mg/ml pepstatin, 1 mg/ml leupeptin, and 1 mg/ml antipain. Protein fractions were separated by SDS-PAGE and electrotransferred onto PVDF membranes. The following primary Abs were used: mouse anti–phosphorylated STAT1 (BD), mouse anti-STAT1 (BD), rabbit anti–phosphorylated STAT3 (Cell Signaling Technology), rabbit anti-STAT3 (Cell Signaling Technology), rabbit anti–phosphorylated STAT4 (Abazyme), rabbit anti-STAT4 (Cell Signaling Technology), mouse anti–α-tubulin (Santa Cruz Biotechnology, Inc.), rabbit anti-TYK2 (C-ter1; Santa Cruz Biotechnology, Inc.), mouse anti-TYK2 (C-ter2; Santa Cruz Biotechnology, Inc.), and mouse anti-TYK2 Abs (N-ter1 [BD] and N-ter2 [a gift from S. Pellegrini, Institut Pasteur, CNRS URA 1961, Paris, France]). Ab binding was detected by incubation with HRP-conjugated anti–mouse or anti–rabbit secondary Abs (GE Healthcare), with the ECL system (Thermo Fisher Scientific).

EMSA. EMSA was performed as previously described (Dupuis et al., 2001). The cells were stimulated with cytokines (at the indicated doses and for the indicated times), and nuclear proteins were extracted. We incubated 10 µg or 15 µg of extract with a ^{32}P-labeled α-dATP (PerkinElmer) probe. Three different probes were used: two gamma interferon activation site (GAS) probes, corresponding to the FcγR1 promoter, 5′-ATGTATTTCCCAGAAA-3′ (for STAT1 and STAT3 binding detection) and 5′-AGCATGTTTCAAGGATTTGAGATGTATTTCCCAGAAAAG-3′ (for STAT4 binding detection), to detect the DNA binding activity of GAFs; and an interferon-stimulated response element (ISRE) probe, corresponding to the promoter of ISG15, 5′-GATCGGGAAAGGGAAACCGAAACTGAA-3′, to detect the DNA-binding activity of ISGF3. DNA binding activity was visualized and measured with a Typhoon Phospho-imager (GE Healthcare). For supershift experiments, we used 2 µg of the following Abs: anti-STAT1 (Santa Cruz Biotechnology, Inc.), anti-STAT2 (Santa Cruz Biotechnology, Inc.), anti-STAT3 (Santa Cruz Biotechnology, Inc.), anti-STAT4.1 (Santa Cruz Biotechnology, Inc.), and anti-STAT4.2 (Invitrogen) Abs.

Production of IFN-γ and IL-12 by *Saimiri* T cells, whole blood, and PBMCs. *Saimiri* T cell lines from patients and controls were starved overnight by incubation in medium containing 1% FBS and were then left unstimulated or were stimulated with 50 ng/ml IL-12 for 48 h or 100 ng/ml IL-23 for 72 h. The secretion of IFN-γ into the culture supernatant was assessed by ELISA (Pelipair) with a Victor X Multilabel Plate Reader (Perkin-Elmer). Whole-blood assays were performed as previously described (Feinberg et al., 2004): heparin-treated blood samples were stimulated in vitro with BCG (multiplicity of infection [MOI] = 20) with or without 5,000 IU/ml IFN-γ or 20 ng/ml IL-12 for 48 h. ELISA was then performed on the collected supernatants, with Abs against IFN-γ or IL-12 (p40 and p70) and the human Pelipair IFN-γ kit (Sanquin) or the human Quantikine HS kit for IL-12 (R&D Systems). The intracellular production of IFN-γ was investigated in PBMCs by flow cytometry. PBMCs (2×10^6 cells/ml) were either left unstimulated or stimulated with BCG (MOI = 20), 100 ng/ml BCG + IL-12 or 25 ng/ml IL-12 + 50 ng/ml IL-18 for 48 h or with 40 ng/ml PMA (Sigma-Aldrich) + 10^{-5} M ionomycin (Sigma-Aldrich) for 24 h, in 12-well plates. All the samples were treated with 1 µg/ml GolgiPlug (BD) for the last 12 h of culture. Supernatants containing suspended PBMCs were collected. After blocking with FcR (Miltenyi Biotec), we performed surface staining with the following Abs: V450 mouse anti–human CD3 (Horizon; BD), PerCP-Cy5.5 mouse anti–human CD19 (BD), and Alexa Fluor 488 mouse anti–human CD56 (BD). We used Aqua (Live/Dead Fixable Dead Cell Stain kit from Invitrogen) staining to exclude dead cells. Intracellular staining was performed with the Cytofix/Cytoperm Plus Fixation/Permeabilization kit (BD). We stained for intracellular IFN-γ with PE mouse anti–human IFN-γ Ab (BD) and for intracellular IL-2 with PE mouse anti–human IL-2 Ab (BD). Compensation was performed on single-stained nonstimulated samples or on single-color stained Compensation Beads (BD). Fluorescence Minus One controls were also included in the experimental design. Staining was assessed on an LSRII flow cytometer (BD), and the results were analyzed with FlowJo (Tree Star).

IL-17$^+$ T cell differentiation ex vivo. The ex vivo detection of human IL-17$^+$ T cells was performed as previously described (de Beaucoudrey et al., 2008). In brief, PBMCs were purified on Ficoll-Paque PLUS (GE Healthcare) and resuspended in RPMI + 10% FBS (Invitrogen). We took aliquots of 10^6 nonadherent cells/ml and either left them unstimulated or stimulated them with 40 ng/ml PMA (Sigma-Aldrich) + 10^{-5} M ionomycin (Sigma-Aldrich) for 12 h. All cells were treated with 1 µl/ml GolgiPlug for the final 12 h of culture. Surface staining was performed with PE-Cy5–conjugated anti–human CD3 (PE Biosciences) Ab, and intracellular staining was performed

with Alexa Fluor 488–conjugated anti–human IL-17 (eBioscience) and PE-conjugated anti–human IFN-γ (BD) or PE-conjugated anti–human IL-22 (R&D Systems) Abs. Cells were analyzed with a FACScan machine and CellQuest software (both from BD).

In vitro differentiation of IL-17$^+$ cells from naive CD4 T cells. Naive (CD45RA$^+$CCR7$^+$) CD4$^+$ T cells were purified from the PBMCs of WT controls (n = 6) or TYK2-deficient patients (P1, P2, and P4) and cultured for 5 d. Cells were exposed to either T cell activation and expansion (TAE) beads (anti-CD2/CD3/CD28) alone or to these beads together with polarizing stimuli to induce the differentiation of Th17 (TGFβ, IL-1β, IL-6, IL-21, IL-23, anti–IL-4, and anti–IFN-γ) type cells. After 5 d, we used cytometric bead assays to assess the secretion of the cytokine indicated in the culture supernatants.

RT-qPCR. Cells were left unstimulated or were stimulated with cytokines (at the indicated doses, for the times stated), and total RNA was extracted with TRIzol. RNA samples were treated with RNase-free DNase (Roche) and cleaned up on an RNeasy column (RNeasy MiniElute Cleanup kit; QIAGEN). Each RNA preparation (1 µg) was reverse transcribed with random hexamers (Applied Biosystems) and the TaqMan Reverse Transcription kit (Applied Biosystems). Transcript levels were determined for *TYK2*, *Mx1*, *ISG15*, *IRF1*, *IFIT1*, and *SOCS3* with TaqMan probes for these genes (Applied Biosystems). Real-time quantitative PCR was performed in an ABI Prism 7500 Sequence Detection System (Applied Biosystems). The results were normalized with respect to the housekeeping gene encoding β-glucuronidase (*GUS*).

Viral assays. Viral assays were performed as previously described (Dupuis et al., 2003). EBV–B cells, *Saimiri* T cells, and SV40-fibroblasts were either left untreated or were treated with 10,000 IU/ml IFN-α for 18 h. We analyzed the growth kinetics of VSV in fibroblasts by incubating the cells with virus-containing medium (MOI = 10) for 30 min, washing twice with PBS, and then culturing the cells in fresh complete medium. Virus-containing supernatants were collected at the time points indicated. We determined the kinetics of VSV and HSV growth in EBV–B and *Saimiri* T cells by resuspending the cells in RPMI medium containing the virus inoculum and incubating for 1 h (VSV MOI = 1, HSV MOI = 0.001), washing with PBS and resuspending in fresh complete medium. Virus-containing supernatants were then collected at the indicated time points. VSV and HSV titers were determined by calculating the 50% end point ($TCID_{50}$), as described by Reed and Muench (1938), after the inoculation of 96-well plates with Vero cell cultures.

Phenotyping of CD4$^+$ and CD8$^+$ T cells. Total PBMCs were labeled with anti-CD4 PE, anti-CD8 PE-Cy7, anti-CD45RA PerCP-Cy5.5, and anti-CCR7 FITC Abs and used for flow cytometry. These Abs bind to cell surface markers, making it possible to identify naive (CCR7$^+$CD45RA$^+$), central memory (CCR7$^+$CD45RA$^-$), and effector memory (CCR7$^-$CD45RA$^-$) CD4$^+$ T cells and naive (CCR7$^+$CD45RA$^+$), central memory (CCR7$^+$CD45RA$^-$), effector memory (CCR7$^-$CD45RA$^-$), and revertant effector memory (CCR7$^-$CD45RA$^+$) CD8$^+$ T cells.

Assessment of STAT3 phosphorylation by flow cytometry. EBV–B cells from the patients and controls were left unstimulated or were stimulated with 100 ng/ml IL-21 for 20 min. The intracellular phosphorylation of STAT3 was assessed by flow cytometry, as described elsewhere (Schulz et al., 2012). We used the Aqua Live/Dead Fixable Dead Cell Stain kit (Invitrogen) to exclude dead cells. Cells were fixed with 1.5% PFA and permeabilized by adding 100% methanol. We then stained them for intracellular tyrosine-phosphorylated STAT3 (pSTAT3), with Alexa Fluor 647 mouse anti–human pSTAT3 (Phosflow; BD), and for the Alexa Fluor 647–coupled isotype.

Silencing in EBV–B cells. EBV–B cells were plated at a concentration of 10^6 cells/ml and infected with retroviral particles at an MOI of 1:1. These particles encoded shRNA1, corresponding to a pool of shRNAs from Sigma-Aldrich, and shRNA2 from Santa Cruz Biotechnology, Inc. Selection was performed with puromycin at a concentration of 0.65 µg/ml, beginning 48 h after transduction.

Expression of receptors at the cell surface. In brief, 0.5 million EBV–B cells were blocked by incubation with 1 µl of FcR blocking reagent in 1% SVF + 1× PBS for 10 min. The Abs were used at a concentration of 125 ng/ml: anti–IFN-γR2–APC (R&D Systems), anti–IFN-γR1–PE (BD), anti–IFN-αR2–PE (PBL), anti–IL-10RB–FITC (R&D Systems), anti-IFNAR1 (AA03; a gift from S. Pellegrini), and anti–IL-12RB1 (BD). They were incubated with the cells for 1 h on ice. The corresponding fluorochrome-conjugated IgG was used as an isotype control. Cells were acquired in LSRII and analyzed with FlowJo software.

ELISA for transcription factors. We assessed the nuclear translocation of STAT3 in response to IL-6 treatment, in a TransAM Transcription Factor ELISA. We used a TransAM STAT3 kit (Active Motif), in accordance with the manufacturer's instructions.

Densitometric analysis and statistics on Western blotting experiments. Semiquantitative analysis of Western blotting experiments was performed with the software ImageJ (NIH). The value of the specific band was divided by the level of housekeeping protein used. The nonstimulated background was removed from the stimulated value. Values were then used to test significance by two-tailed Student's t test.

Online supplemental material. Fig. S1 shows impaired IL-12 responses in TYK2-deficient patients. Table S1 summarizes the functional experiments performed in TYK2-deficient cells. Online supplemental material is available at http://www.jem.org/cgi/content/full/jem.20140280/DC1.

We would like to thank the patients, their relatives, and their physicians. We also thank Vanessa Bryant, Yelena Nemirovskaya, Tatiana Kochetkov, Lazaro Lorenzo-Diaz, Hye Kyung Lim, Sophie Cypowyj, and Svetlana Mazel and her team at the Rockefeller University Flow Cytometry Resource Center. We would like to thank Sandra Pellegrini for generously providing us with a TYK2 Ab.

The Laboratory of Human Genetics of Infectious Diseases was supported in part by grants from the French National Agency for Research (ANR), the EU-grant HOMITB (HEALTH-F3-2008-200732), the European Research Council (ERC; ERC-2010-AdG-268777), the Bill and Melinda Gates Foundation, the St. Giles Foundation, the Jeffrey Modell Foundation and Talecris Biotherapeutics, the National Center for Research Resources and the National Center for Advancing Sciences (NCATS), National Institutes of Health grant 8UL1TR000043, the National Institute of Allergy and Infectious Diseases (NIAID) grants 5R01AI089970, 5R37AI095983, and 5U01AI088685, and The Rockefeller University. A.Y. Kreins was supported by Fondation Médicale Medische Stichting Mathilde E. Horlait-Dapsens, D. Bogunovic by the Helmsley Fellowship for Basic and Translational Research on Disorders of the Digestive System and NIAID grant 1K99AI106942, X.-F. Kong by the Stony Wold-Herbert Fund, and R. Martinez-Barricarte by the European Molecular Biology Organization (EMBO). C.S. Ma and S.G. Tangye are supported by fellowships and grants from the National Health and Medical Research Council of Australia. The work of S. Rose-John was supported by the Deutsche Forschungsgemeinschaft (DFG), Bonn (SFB841, project C1; SFB877, project A1), and by the Cluster of Excellence "Inflammation at interfaces."

The authors declare no competing financial interests.

Submitted: 11 February 2014
Accepted: 4 August 2015

REFERENCES

Altare, F., A. Durandy, D. Lammas, J.F. Emile, S. Lamhamedi, F. Le Deist, P. Drysdale, E. Jouanguy, R. Döffinger, F. Bernaudin, et al. 1998. Impairment of mycobacterial immunity in human interleukin-12 receptor deficiency. *Science*. 280:1432–1435. http://dx.doi.org/10.1126/science.280.5368.1432

Altare, F., A. Ensser, A. Breiman, J. Reichenbach, J.E. Baghdadi, A. Fischer, J.F. Emile, J.L. Gaillard, E. Meinl, and J.L. Casanova. 2001. Interleukin-12

receptor β1 deficiency in a patient with abdominal tuberculosis. *J. Infect. Dis.* 184:231–236. http://dx.doi.org/10.1086/321999

Beşer, O.F., C.D. Conde, T. Kutlu, F.C. Cokuğraş, K. Boztuğ, and T. Erkan. 2014. Inflammatory bowel disease with lethal disease course caused by a nonsense mutation in BIRC4 encoding X-linked inhibitor of apoptosis protein (XIAP). *J. Pediatr. Gastroenterol. Nutr.* In press.

Boisson, B., C. Wang, V. Pedergnana, L. Wu, S. Cypowyj, M. Rybojad, A. Belkadi, C. Picard, L. Abel, C. Fieschi, et al. 2013. An ACT1 mutation selectively abolishes interleukin-17 responses in humans with chronic mucocutaneous candidiasis. *Immunity*. 39:676–686. http://dx.doi.org/10.1016/j.immuni.2013.09.002

Boisson-Dupuis, S., J. El Baghdadi, N. Parvaneh, A. Bousfiha, J. Bustamante, J. Feinberg, A. Samarina, A.V. Grant, L. Janniere, N. El Hafidi, et al. 2011. IL-12Rβ1 deficiency in two of fifty children with severe tuberculosis from Iran, Morocco, and Turkey. *PLoS ONE*. 6:e18524. http://dx.doi.org/10.1371/journal.pone.0018524

Boisson-Dupuis, S., X.F. Kong, S. Okada, S. Cypowyj, A. Puel, L. Abel, and J.L. Casanova. 2012. Inborn errors of human STAT1: allelic heterogeneity governs the diversity of immunological and infectious phenotypes. *Curr. Opin. Immunol.* 24:364–378. http://dx.doi.org/10.1016/j.coi.2012.04.011

Boisson-Dupuis, S., J. Bustamante, J. El-Baghdadi, Y. Camcioglu, N. Parvaneh, S. El Azbaoui, A. Agader, A. Hassani, N. El Hafidi, N.A. Mrani, et al. 2015. Inherited and acquired immunodeficiencies underlying tuberculosis in childhood. *Immunol. Rev.* 264:103–120. http://dx.doi.org/10.1111/imr.12272

Bustamante, J., S. Boisson-Dupuis, L. Abel, and J.L. Casanova. 2014. Mendelian susceptibility to mycobacterial disease: genetic, immunological, and clinical features of inborn errors of IFN-γ immunity. *Semin. Immunol.* 26:454–470. http://dx.doi.org/10.1016/j.smim.2014.09.008

Byun, M., A. Abhyankar, V. Lelarge, S. Plancoulaine, A. Palanduz, L. Telhan, B. Boisson, C. Picard, S. Dewell, C. Zhao, et al. 2010. Whole-exome sequencing-based discovery of STIM1 deficiency in a child with fatal classic Kaposi sarcoma. *J. Exp. Med.* 207:2307–2312. http://dx.doi.org/10.1084/jem.20101597

Casanova, J.L., and L. Abel. 2002. Genetic dissection of immunity to mycobacteria: the human model. *Annu. Rev. Immunol.* 20:581–620. http://dx.doi.org/10.1146/annurev.immunol.20.081501.125851

Casanova, J.L., and L. Abel. 2013. The genetic theory of infectious diseases: a brief history and selected illustrations. *Annu. Rev. Genomics Hum. Genet.* 14:215–243. http://dx.doi.org/10.1146/annurev-genom-091212-153448

Casanova, J.L., S.M. Holland, and L.D. Notarangelo. 2012. Inborn errors of human JAKs and STATs. *Immunity*. 36:515–528. http://dx.doi.org/10.1016/j.immuni.2012.03.016

Casanova, J.L., L. Abel, and L. Quintana-Murci. 2013. Immunology taught by human genetics. *Cold Spring Harb. Symp. Quant. Biol.* 78:157–172. http://dx.doi.org/10.1101/sqb.2013.78.019968

Casanova, J.L., M.E. Conley, S.J. Seligman, L. Abel, and L.D. Notarangelo. 2014. Guidelines for genetic studies in single patients: lessons from primary immunodeficiencies. *J. Exp. Med.* 211:2137–2149. http://dx.doi.org/10.1084/jem.20140520

Chandesris, M.O., I. Melki, A. Natividad, A. Puel, C. Fieschi, L. Yun, C. Thumerelle, E. Oksenhendler, D. Boutboul, C. Thomas, et al. 2012. Autosomal dominant STAT3 deficiency and hyper-IgE syndrome: molecular, cellular, and clinical features from a French national survey. *Medicine (Baltimore)*. 91:e1–e19. http://dx.doi.org/10.1097/MD.0b013e31825f95b9

Chapgier, A., R.F. Wynn, E. Jouanguy, O. Filipe-Santos, S. Zhang, J. Feinberg, K. Hawkins, J.L. Casanova, and P.D. Arkwright. 2006. Human complete Stat-1 deficiency is associated with defective type I and II IFN responses in vitro but immunity to some low virulence viruses in vivo. *J. Immunol.* 176:5078–5083. http://dx.doi.org/10.4049/jimmunol.176.8.5078

Chapgier, A., X.F. Kong, S. Boisson-Dupuis, E. Jouanguy, D. Averbuch, J. Feinberg, S.Y. Zhang, J. Bustamante, G. Vogt, J. Lejeune, et al. 2009. A partial form of recessive STAT1 deficiency in humans. *J. Clin. Invest.* 119:1502–1514. http://dx.doi.org/10.1172/JCI37083

Cole, N., S. Bao, F. Stapleton, A. Thakur, A.J. Husband, K.W. Beagley, and M.D. Willcox. 2003. *Pseudomonas aeruginosa* keratitis in IL-6-deficient mice. *Int. Arch. Allergy Immunol.* 130:165–172. http://dx.doi.org/10.1159/000069006

Dalrymple, S.A., R. Slattery, D.M. Aud, M. Krishna, L.A. Lucian, and R. Murray. 1996. Interleukin-6 is required for a protective immune response to systemic *Escherichia coli* infection. *Infect. Immun.* 64:3231–3235.

de Beaucoudrey, L., A. Puel, O. Filipe-Santos, A. Cobat, P. Ghandil, M. Chrabieh, J. Feinberg, H. von Bernuth, A. Samarina, L. Jannière, et al. 2008. Mutations in *STAT3* and *IL12RB1* impair the development of human IL-17–producing T cells. *J. Exp. Med.* 205:1543–1550. http://dx.doi.org/10.1084/jem.20080321

de Beaucoudrey, L., A. Samarina, J. Bustamante, A. Cobat, S. Boisson-Dupuis, J. Feinberg, S. Al-Muhsen, L. Jannière, Y. Rose, M. de Suremain, et al. 2010. Revisiting human IL-12Rβ1 deficiency: a survey of 141 patients from 30 countries. *Medicine (Baltimore)*. 89:381–402. http://dx.doi.org/10.1097/MD.0b013e3181fdd832

Diao, H., and M. Kohanawa. 2005. Endogenous interleukin-6 plays a crucial protective role in streptococcal toxic shock syndrome via suppression of tumor necrosis factor alpha production. *Infect. Immun.* 73:3745–3748. http://dx.doi.org/10.1128/IAI.73.6.3745-3748.2005

Dupuis, S., C. Dargemont, C. Fieschi, N. Thomassin, S. Rosenzweig, J. Harris, S.M. Holland, R.D. Schreiber, and J.L. Casanova. 2001. Impairment of mycobacterial but not viral immunity by a germline human STAT1 mutation. *Science*. 293:300–303. http://dx.doi.org/10.1126/science.1061154

Dupuis, S., E. Jouanguy, S. Al-Hajjar, C. Fieschi, I.Z. Al-Mohsen, S. Al-Jumaah, K. Yang, A. Chapgier, C. Eidenschenk, P. Eid, et al. 2003. Impaired response to interferon-α/β and lethal viral disease in human STAT1 deficiency. *Nat. Genet.* 33:388–391. http://dx.doi.org/10.1038/ng1097

Elsaesser, H., K. Sauer, and D.G. Brooks. 2009. IL-21 is required to control chronic viral infection. *Science*. 324:1569–1572. http://dx.doi.org/10.1126/science.1174182

Feinberg, J., C. Fieschi, R. Doffinger, M. Feinberg, T. Leclerc, S. Boisson-Dupuis, C. Picard, J. Bustamante, A. Chapgier, O. Filipe-Santos, et al. 2004. Bacillus Calmette Guérin triggers the IL-12/IFN-γ axis by an IRAK-4- and NEMO-dependent, non-cognate interaction between monocytes, NK, and T lymphocytes. *Eur. J. Immunol.* 34:3276–3284. http://dx.doi.org/10.1002/eji.200425221

Fieschi, C., S. Dupuis, E. Catherinot, J. Feinberg, J. Bustamante, A. Breiman, F. Altare, R. Baretto, F. Le Deist, S. Kayal, et al. 2003. Low penetrance, broad resistance, and favorable outcome of interleukin 12 receptor β1 deficiency: medical and immunological implications. *J. Exp. Med.* 197:527–535. http://dx.doi.org/10.1084/jem.20021769

Fischer, M., J. Goldschmitt, C. Peschel, J.P. Brakenhoff, K.J. Kallen, A. Wollmer, J. Grötzinger, and S. Rose-John. 1997. I. A bioactive designer cytokine for human hematopoietic progenitor cell expansion. *Nat. Biotechnol.* 15:142–145. http://dx.doi.org/10.1038/nbt0297-142

Foulds, K.E., M.J. Rotte, and R.A. Seder. 2006. IL-10 is required for optimal CD8 T cell memory following *Listeria monocytogenes* infection. *J. Immunol.* 177:2565–2574. http://dx.doi.org/10.4049/jimmunol.177.4.2565

Fröhlich, A., J. Kisielow, I. Schmitz, S. Freigang, A.T. Shamshiev, J. Weber, B.J. Marsland, A. Oxenius, and M. Kopf. 2009. IL-21R on T cells is critical for sustained functionality and control of chronic viral infection. *Science*. 324:1576–1580. http://dx.doi.org/10.1126/science.1172815

Ghoreschi, K., A. Laurence, and J.J. O'Shea. 2009. Janus kinases in immune cell signaling. *Immunol. Rev.* 228:273–287. http://dx.doi.org/10.1111/j.1600-065X.2008.00754.x

Glocker, E.O., D. Kotlarz, K. Boztug, E.M. Gertz, A.A. Schäffer, F. Noyan, M. Perro, J. Diestelhorst, A. Allroth, D. Murugan, et al. 2009. Inflammatory bowel disease and mutations affecting the interleukin-10 receptor. *N. Engl. J. Med.* 361:2033–2045. http://dx.doi.org/10.1056/NEJMoa0907206

Glocker, E.O., N. Frede, M. Perro, N. Sebire, M. Elawad, N. Shah, and B. Grimbacher. 2010. Infant colitis—it's in the genes. *Lancet*. 376:1272. http://dx.doi.org/10.1016/S0140-6736(10)61008-2

Glocker, E.O., D. Kotlarz, C. Klein, N. Shah, and B. Grimbacher. 2011. IL-10 and IL-10 receptor defects in humans. *Ann. N. Y. Acad. Sci.* 1246:102–107. http://dx.doi.org/10.1111/j.1749-6632.2011.06339.x

Grant, A.V., S. Boisson-Dupuis, E. Herquelot, L. de Beaucoudrey, O. Filipe-Santos, D.K. Nolan, J. Feinberg, A. Boland, S. Al-Muhsen, O. Sanal, et al. 2011. Accounting for genetic heterogeneity in homozygosity mapping: application to Mendelian susceptibility to mycobacterial disease. *J. Med. Genet.* 48:567–571. http://dx.doi.org/10.1136/jmg.2011.089128

Grimbacher, B., S.M. Holland, J.I. Gallin, F. Greenberg, S.C. Hill, H.L. Malech, J.A. Miller, A.C. O'Connell, and J.M. Puck. 1999. Hyper-IgE syndrome with recurrent infections—an autosomal dominant multisystem disorder. *N. Engl. J. Med.* 340:692–702. http://dx.doi.org/10.1056/NEJM199903043400904

Guschin, D., N. Rogers, J. Briscoe, B. Witthuhn, D. Watling, F. Horn, S. Pellegrini, K. Yasukawa, P. Heinrich, G.R. Stark, et al. 1995. A major role for the protein tyrosine kinase JAK1 in the JAK/STAT signal transduction pathway in response to interleukin-6. *EMBO J.* 14:1421–1429.

Hambleton, S., S. Goodbourn, D.F. Young, P. Dickinson, S.M. Mohamad, M. Valappil, N. McGovern, A.J. Cant, S.J. Hackett, P. Ghazal, et al. 2013. STAT2 deficiency and susceptibility to viral illness in humans. *Proc. Natl. Acad. Sci. USA.* 110:3053–3058. http://dx.doi.org/10.1073/pnas.1220098110

Heimall, J., A. Freeman, and S.M. Holland. 2010. Pathogenesis of hyper IgE syndrome. *Clin. Rev. Allergy Immunol.* 38:32–38. http://dx.doi.org/10.1007/s12016-009-8134-1

Holland, S.M., F.R. DeLeo, H.Z. Elloumi, A.P. Hsu, G. Uzel, N. Brodsky, A.F. Freeman, A. Demidowich, J. Davis, M.L. Turner, et al. 2007. STAT3 mutations in the hyper-IgE syndrome. *N. Engl. J. Med.* 357:1608–1619. http://dx.doi.org/10.1056/NEJMoa073687

Hume, E.B., N. Cole, L.L. Garthwaite, S. Khan, and M.D. Willcox. 2006. A protective role for IL-6 in staphylococcal microbial keratitis. *Invest. Ophthalmol. Vis. Sci.* 47:4926–4930. http://dx.doi.org/10.1167/iovs.06-0340

Ihle, J.N. 1995. The Janus protein tyrosine kinases in hematopoietic cytokine signaling. *Semin. Immunol.* 7:247–254. http://dx.doi.org/10.1006/smim.1995.0029

Ihle, J.N., and I.M. Kerr. 1995. Jaks and Stats in signaling by the cytokine receptor superfamily. *Trends Genet.* 11:69–74. http://dx.doi.org/10.1016/S0168-9525(00)89000-9

Ishizaki, M., R. Muromoto, T. Akimoto, Y. Ohshiro, M. Takahashi, Y. Sekine, H. Maeda, K. Shimoda, K. Oritani, and T. Matsuda. 2011. Tyk2 deficiency protects joints against destruction in anti-type II collagen antibody-induced arthritis in mice. *Int. Immunol.* 23:575–582. http://dx.doi.org/10.1093/intimm/dxr057

Itan, Y., S.Y. Zhang, G. Vogt, A. Abhyankar, M. Herman, P. Nitschke, D. Fried, L. Quintana-Murci, L. Abel, and J.L. Casanova. 2013. The human gene connectome as a map of short cuts for morbid allele discovery. *Proc. Natl. Acad. Sci. USA.* 110:5558–5563. http://dx.doi.org/10.1073/pnas.1218167110

Itan, Y., M. Mazel, B. Mazel, A. Abhyankar, P. Nitschke, L. Quintana-Murci, S. Boisson-Dupuis, B. Boisson, L. Abel, S.Y. Zhang, and J.L. Casanova. 2014. HGCS: an online tool for prioritizing disease-causing gene variants by biological distance. *BMC Genomics.* 15:256. http://dx.doi.org/10.1186/1471-2164-15-256

Ives, M.L., C.S. Ma, U. Palendira, A. Chan, J. Bustamante, S. Boisson-Dupuis, P.D. Arkwright, D. Engelhard, D. Averbuch, K. Magdorf, et al. 2013. Signal transducer and activator of transcription 3 (STAT3) mutations underlying autosomal dominant hyper-IgE syndrome impair human $CD8^+$ T-cell memory formation and function. *J. Allergy Clin. Immunol.* 132:400–411. http://dx.doi.org/10.1016/j.jaci.2013.05.029

Jones, M.R., L.J. Quinton, B.T. Simms, M.M. Lupa, M.S. Kogan, and J.P. Mizgerd. 2006. Roles of interleukin-6 in activation of STAT proteins and recruitment of neutrophils during *Escherichia coli* pneumonia. *J. Infect. Dis.* 193:360–369. http://dx.doi.org/10.1086/499312

Jouanguy, E., S.Y. Zhang, A. Chapgier, V. Sancho-Shimizu, A. Puel, C. Picard, S. Boisson-Dupuis, L. Abel, and J.L. Casanova. 2007. Human primary immunodeficiencies of type I interferons. *Biochimie.* 89:878–883. http://dx.doi.org/10.1016/j.biochi.2007.04.016

Karaghiosoff, M., H. Neubauer, C. Lassnig, P. Kovarik, H. Schindler, H. Pircher, B. McCoy, C. Bogdan, T. Decker, G. Brem, et al. 2000. Partial impairment of cytokine responses in Tyk2-deficient mice. *Immunity.* 13:549–560. http://dx.doi.org/10.1016/S1074-7613(00)00054-6

Kilic, S.S., M. Hacimustafaoglu, S. Boisson-Dupuis, A.Y. Kreins, A.V. Grant, L. Abel, and J.L. Casanova. 2012. A patient with tyrosine kinase 2 deficiency without hyper-IgE syndrome. *J. Pediatr.* 160:1055–1057. http://dx.doi.org/10.1016/j.jpeds.2012.01.056

Kong, X.F., M. Ciancanelli, S. Al-Hajjar, L. Alsina, T. Zumwalt, J. Bustamante, J. Feinberg, M. Audry, C. Prando, V. Bryant, et al. 2010. A novel form of human STAT1 deficiency impairing early but not late responses to interferons. *Blood.* 116:5895–5906. http://dx.doi.org/10.1182/blood-2010-04-280586

Kotenko, S.V., and J.A. Langer. 2004. Full house: 12 receptors for 27 cytokines. *Int. Immunopharmacol.* 4:593–608. http://dx.doi.org/10.1016/j.intimp.2004.01.003

Kotenko, S.V., G. Gallagher, V.V. Baurin, A. Lewis-Antes, M. Shen, N.K. Shah, J.A. Langer, F. Sheikh, H. Dickensheets, and R.P. Donnelly. 2003. IFN-lambdas mediate antiviral protection through a distinct class II cytokine receptor complex. *Nat. Immunol.* 4:69–77. http://dx.doi.org/10.1038/ni875

Kotlarz, D., N. Zięt ara, G. Uzel, T. Weidemann, C.J. Braun, J. Diestelhorst, P.M. Krawitz, P.N. Robinson, J. Hecht, J. Puchałka, et al. 2013. Loss-of-function mutations in the IL-21 receptor gene cause a primary immunodeficiency syndrome. *J. Exp. Med.* 210:433–443. http://dx.doi.org/10.1084/jem.20111229

Kotlarz, D., N. Zięt ara, J.D. Milner, and C. Klein. 2014. Human IL-21 and IL-21R deficiencies: two novel entities of primary immunodeficiency. *Curr. Opin. Pediatr.* 26:704–712. http://dx.doi.org/10.1097/MOP.0000000000000160

Leonard, W.J., and J.J. O'Shea. 1998. Jaks and STATs: biological implications. *Annu. Rev. Immunol.* 16:293–322. http://dx.doi.org/10.1146/annurev.immunol.16.1.293

Ling, Y., S. Cypowyj, C. Aytekin, M. Galicchio, Y. Camcioglu, S. Nepesov, A. Ikinciogullari, F. Dogu, A. Belkadi, R. Levy, et al. 2015. Inherited IL-17RC deficiency in patients with chronic mucocutaneous candidiasis. *J. Exp. Med.* 212:619–631. http://dx.doi.org/10.1084/jem.20141065

Liu, L., S. Okada, X.F. Kong, A.Y. Kreins, S. Cypowyj, A. Abhyankar, J. Toubiana, Y. Itan, M. Audry, P. Nitschke, et al. 2011. Gain-of-function human STAT1 mutations impair IL-17 immunity and underlie chronic mucocutaneous candidiasis. *J. Exp. Med.* 208:1635–1648. http://dx.doi.org/10.1084/jem.20110958

Ma, C.S., G.Y. Chew, N. Simpson, A. Priyadarshi, M. Wong, B. Grimbacher, D.A. Fulcher, S.G. Tangye, and M.C. Cook. 2008. Deficiency of Th17 cells in hyper IgE syndrome due to mutations in STAT3. *J. Exp. Med.* 205:1551–1557. http://dx.doi.org/10.1084/jem.20080218

Ma, C.S., D.T. Avery, A. Chan, M. Batten, J. Bustamante, S. Boisson-Dupuis, P.D. Arkwright, A.Y. Kreins, D. Averbuch, D. Engelhard, et al. 2012. Functional STAT3 deficiency compromises the generation of human T follicular helper cells. *Blood.* 119:3997–4008. http://dx.doi.org/10.1182/blood-2011-11-392985

Mao, H., W. Yang, P.P. Lee, M.H. Ho, J. Yang, S. Zeng, C.Y. Chong, T.L. Lee, W. Tu, and Y.L. Lau. 2012. Exome sequencing identifies novel compound heterozygous mutations of IL-10 receptor 1 in neonatal-onset Crohn's disease. *Genes Immun.* 13:437–442. http://dx.doi.org/10.1038/gene.2012.8

Minegishi, Y. 2009. Hyper-IgE syndrome. *Curr. Opin. Immunol.* 21:487–492. http://dx.doi.org/10.1016/j.coi.2009.07.013

Minegishi, Y., M. Saito, T. Morio, K. Watanabe, K. Agematsu, S. Tsuchiya, H. Takada, T. Hara, N. Kawamura, T. Ariga, et al. 2006. Human tyrosine kinase 2 deficiency reveals its requisite roles in multiple cytokine signals involved in innate and acquired immunity. *Immunity.* 25:745–755. http://dx.doi.org/10.1016/j.immuni.2006.09.009

Minegishi, Y., M. Saito, S. Tsuchiya, I. Tsuge, H. Takada, T. Hara, N. Kawamura, T. Ariga, S. Pasic, O. Stojkovic, et al. 2007. Dominant-negative mutations in the DNA-binding domain of STAT3 cause hyper-IgE syndrome. *Nature.* 448:1058–1062. http://dx.doi.org/10.1038/nature06096

Nanki, T., I. Onoue, K. Nagasaka, A. Takayasu, M. Ebisawa, T. Hosoya, T. Shirai, T. Sugihara, S. Hirata, T. Kubota, et al. 2013. Suppression of elevations in serum C reactive protein levels by anti-IL-6 autoantibodies in two patients with severe bacterial infections. *Ann. Rheum. Dis.* 72:1100–1102. http://dx.doi.org/10.1136/annrheumdis-2012-202768

Ortmann, R., R. Smeltz, G. Yap, A. Sher, and E.M. Shevach. 2001. A heritable defect in IL-12 signaling in B10.Q/J mice. I. In vitro analysis. *J. Immunol.* 166:5712–5719. http://dx.doi.org/10.4049/jimmunol.166.9.5712

Ouederni, M., O. Sanal, A. Ikinciogullari, I. Tezcan, F. Dogu, I. Sologuren, S. Pedraza-Sánchez, M. Keser, G. Tanir, C. Nieuwhof, et al. 2014. Clinical features of Candidiasis in patients with inherited interleukin 12 receptor β1 deficiency. *Clin. Infect. Dis.* 58:204–213. http://dx.doi.org/10.1093/cid/cit722

Paulson, M.L., A.F. Freeman, and S.M. Holland. 2008. Hyper IgE syndrome: an update on clinical aspects and the role of signal transducer and activator of transcription 3. *Curr. Opin. Allergy Clin. Immunol.* 8:527–533. http://dx.doi.org/10.1097/ACI.0b013e3283184210

Pellegrini, M., T. Calzascia, J.G. Toe, S.P. Preston, A.E. Lin, A.R. Elford, A. Shahinian, P.A. Lang, K.S. Lang, M. Morre, et al. 2011. IL-7 engages multiple mechanisms to overcome chronic viral infection and limit organ pathology. *Cell.* 144:601–613. http://dx.doi.org/10.1016/j.cell.2011.01.011

Pestka, S., C.D. Krause, and M.R. Walter. 2004. Interferons, interferon-like cytokines, and their receptors. *Immunol. Rev.* 202:8–32. http://dx.doi.org/10.1111/j.0105-2896.2004.00204.x

Prchal-Murphy, M., C. Semper, C. Lassnig, B. Wallner, C. Gausterer, I. Teppner-Klymiuk, J. Kobolak, S. Müller, T. Kolbe, M. Karaghiosoff, et al. 2012. TYK2 kinase activity is required for functional type I interferon responses in vivo. *PLoS ONE.* 7:e39141. http://dx.doi.org/10.1371/journal.pone.0039141

Puel, A., C. Picard, M. Lorrot, C. Pons, M. Chrabieh, L. Lorenzo, M. Mamani-Matsuda, E. Jouanguy, D. Gendrel, and J.L. Casanova. 2008. Recurrent staphylococcal cellulitis and subcutaneous abscesses in a child with autoantibodies against IL-6. *J. Immunol.* 180:647–654. http://dx.doi.org/10.4049/jimmunol.180.1.647

Puel, A., S. Cypowyj, J. Bustamante, J.F. Wright, L. Liu, H.K. Lim, M. Migaud, L. Israel, M. Chrabieh, M. Audry, et al. 2011. Chronic mucocutaneous candidiasis in humans with inborn errors of interleukin-17 immunity. *Science.* 332:65–68. http://dx.doi.org/10.1126/science.1200439

Ragimbeau, J., E. Dondi, A. Alcover, P. Eid, G. Uzé, and S. Pellegrini. 2003. The tyrosine kinase Tyk2 controls IFNAR1 cell surface expression. *EMBO J.* 22:537–547. http://dx.doi.org/10.1093/emboj/cdg038

Rani, M.R., D.W. Leaman, Y. Han, S. Leung, E. Croze, E.N. Fish, A. Wolfman, and R.M. Ransohoff. 1999. Catalytically active TYK2 is essential for interferon-β-mediated phosphorylation of STAT3 and interferon-α receptor-1 (IFNAR-1) but not for activation of phosphoinositol 3-kinase. *J. Biol. Chem.* 274:32507–32511. http://dx.doi.org/10.1074/jbc.274.45.32507

Reed, L.J., and H. Muench. 1938. A simple method of estimating fifty per cent endpoint. *Am. J. Hyg.* 27:493–497.

Rosenzweig, S.D., and S.M. Holland. 2011. Recent insights into the pathobiology of innate immune deficiencies. *Curr. Allergy Asthma Rep.* 11:369–377. http://dx.doi.org/10.1007/s11882-011-0212-9

Saito, M., M. Nagasawa, H. Takada, T. Hara, S. Tsuchiya, K. Agematsu, M. Yamada, N. Kawamura, T. Ariga, I. Tsuge, et al. 2011. Defective IL-10 signaling in hyper-IgE syndrome results in impaired generation of tolerogenic dendritic cells and induced regulatory T cells. *J. Exp. Med.* 208:235–249. http://dx.doi.org/10.1084/jem.20100799

Schulz, K.R., E.A. Danna, P.O. Krutzik, and G.P. Nolan. 2012. Single-cell phospho-protein analysis by flow cytometry. *Curr. Protoc. Immunol.* Chapter 8:1–20. http://dx.doi.org/10.1002/0471142735.im0817s96

Shaw, M.H., V. Boyartchuk, S. Wong, M. Karaghiosoff, J. Ragimbeau, S. Pellegrini, M. Muller, W.F. Dietrich, and G.S. Yap. 2003. A natural mutation in the Tyk2 pseudokinase domain underlies altered susceptibility of B10.Q/J mice to infection and autoimmunity. *Proc. Natl. Acad. Sci. USA.* 100:11594–11599. http://dx.doi.org/10.1073/pnas.1930781100

Shimoda, K., K. Kato, K. Aoki, T. Matsuda, A. Miyamoto, M. Shibamori, M. Yamashita, A. Numata, K. Takase, S. Kobayashi, et al. 2000. Tyk2 plays a restricted role in IFNα signaling, although it is required for IL-12-mediated T cell function. *Immunity.* 13:561–571. http://dx.doi.org/10.1016/S1074-7613(00)00055-8

Shimoda, K., H. Tsutsui, K. Aoki, K. Kato, T. Matsuda, A. Numata, K. Takase, T. Yamamoto, H. Nukina, T. Hoshino, et al. 2002. Partial impairment of interleukin-12 (IL-12) and IL-18 signaling in Tyk2-deficient mice. *Blood.* 99:2094–2099. http://dx.doi.org/10.1182/blood.V99.6.2094

Siegel, A.M., J. Heimall, A.F. Freeman, A.P. Hsu, E. Brittain, J.M. Brenchley, D.C. Douek, G.H. Fahle, J.I. Cohen, S.M. Holland, and J.D. Milner. 2011. A critical role for STAT3 transcription factor signaling in the development and maintenance of human T cell memory. *Immunity.* 35:806–818. http://dx.doi.org/10.1016/j.immuni.2011.09.016

Sohn, S.J., K. Barrett, A. Van Abbema, C. Chang, P.B. Kohli, H. Kanda, J. Smith, Y. Lai, A. Zhou, B. Zhang, et al. 2013. A restricted role for TYK2 catalytic activity in human cytokine responses revealed by novel TYK2-selective inhibitors. *J. Immunol.* 191:2205–2216. http://dx.doi.org/10.4049/jimmunol.1202859

Sowerwine, K.J., S.M. Holland, and A.F. Freeman. 2012. Hyper-IgE syndrome update. *Ann. N. Y. Acad. Sci.* 1250:25–32. http://dx.doi.org/10.1111/j.1749-6632.2011.06387.x

Stahl, N., T.G. Boulton, T. Farruggella, N.Y. Ip, S. Davis, B.A. Witthuhn, F.W. Quelle, O. Silvennoinen, G. Barbieri, S. Pellegrini, et al. 1994. Association and activation of Jak-Tyk kinases by CNTF-LIF-OSM-IL-6 beta receptor components. *Science.* 263:92–95. http://dx.doi.org/10.1126/science.8272873

Stark, G.R., and J.E. Darnell Jr. 2012. The JAK-STAT pathway at twenty. *Immunity.* 36:503–514. http://dx.doi.org/10.1016/j.immuni.2012.03.013

Stark, G.R., I.M. Kerr, B.R. Williams, R.H. Silverman, and R.D. Schreiber. 1998. How cells respond to interferons. *Annu. Rev. Biochem.* 67:227–264. http://dx.doi.org/10.1146/annurev.biochem.67.1.227

Stoddard, J.L., J.E. Niemela, T.A. Fleisher, and S.D. Rosenzweig. 2014. Targeted NGS: A cost-effective approach to molecular diagnosis of PIDs. *Front. Immunol.* 5:531. http://dx.doi.org/10.3389/fimmu.2014.00531

Strobl, B., D. Stoiber, V. Sexl, and M. Mueller. 2011. Tyrosine kinase 2 (TYK2) in cytokine signalling and host immunity. *Front Biosci (Landmark Ed).* 16:3214–3232. http://dx.doi.org/10.2741/3908

Taga, T., M. Hibi, Y. Hirata, K. Yamasaki, K. Yasukawa, T. Matsuda, T. Hirano, and T. Kishimoto. 1989. Interleukin-6 triggers the association of its receptor with a possible signal transducer, gp130. *Cell.* 58:573–581. http://dx.doi.org/10.1016/0092-8674(89)90438-8

Tangye, S.G. 2015. Advances in IL-21 biology - enhancing our understanding of human disease. *Curr. Opin. Immunol.* 34:107–115. http://dx.doi.org/10.1016/j.coi.2015.02.010

Tokumasa, N., A. Suto, S. Kagami, S. Furuta, K. Hirose, N. Watanabe, Y. Saito, K. Shimoda, I. Iwamoto, and H. Nakajima. 2007. Expression of Tyk2 in dendritic cells is required for IL-12, IL-23, and IFN-γ production and the induction of Th1 cell differentiation. *Blood.* 110:553–560. http://dx.doi.org/10.1182/blood-2006-11-059246

Vairo, D., L. Tassone, G. Tabellini, N. Tamassia, S. Gasperini, F. Bazzoni, A. Plebani, F. Porta, L.D. Notarangelo, S. Parolini, et al. 2011. Severe impairment of IFN-γ and IFN-α responses in cells of a patient with a novel STAT1 splicing mutation. *Blood.* 118:1806–1817. http://dx.doi.org/10.1182/blood-2011-01-330571

van de Veerdonk, F.L., T.S. Plantinga, A. Hoischen, S.P. Smeekens, L.A. Joosten, C. Gilissen, P. Arts, D.C. Rosentul, A.J. Carmichael, C.A. Smits-van der Graaf, et al. 2011. STAT1 mutations in autosomal dominant chronic mucocutaneous candidiasis. *N. Engl. J. Med.* 365:54–61. http://dx.doi.org/10.1056/NEJMoa1100102

van der Poll, T., C.V. Keogh, X. Guirao, W.A. Buurman, M. Kopf, and S.F. Lowry. 1997. Interleukin-6 gene-deficient mice show impaired defense against pneumococcal pneumonia. *J. Infect. Dis.* 176:439–444. http://dx.doi.org/10.1086/514062

van Enckevort, F.H., C.G. Sweep, P.N. Span, M.G. Netea, A.R. Hermus, and B.J. Kullberg. 2001. Reduced adrenal response and increased mortality after systemic *Klebsiella pneumoniae* infection in interleukin-6-deficient mice. *Eur. Cytokine Netw.* 12:581–586.

Velazquez, L., M. Fellous, G.R. Stark, and S. Pellegrini. 1992. A protein tyrosine kinase in the interferon α/β signaling pathway. *Cell.* 70:313–322. http://dx.doi.org/10.1016/0092-8674(92)90105-L

Velazquez, L., K.E. Mogensen, G. Barbieri, M. Fellous, G. Uzé, and S. Pellegrini. 1995. Distinct domains of the protein tyrosine kinase tyk2 required for binding of interferon-α/β and for signal transduction. *J. Biol. Chem.* 270:3327–3334. http://dx.doi.org/10.1074/jbc.270.7.3327

Watford, W.T., B.D. Hissong, J.H. Bream, Y. Kanno, L. Muul, and J.J. O'Shea. 2004. Signaling by IL-12 and IL-23 and the immunoregulatory roles of STAT4. *Immunol. Rev.* 202:139–156. http://dx.doi.org/10.1111/j.0105-2896.2004.00211.x

Yap, G.S., R. Ortmann, E. Shevach, and A. Sher. 2001. A heritable defect in IL-12 signaling in B10.Q/J mice. II. Effect on acute resistance to *Toxoplasma gondii* and rescue by IL-18 treatment. *J. Immunol.* 166:5720–5725. http://dx.doi.org/10.4049/jimmunol.166.9.5720

Yi, J.S., M. Du, and A.J. Zajac. 2009. A vital role for interleukin-21 in the control of a chronic viral infection. *Science*. 324:1572–1576. http://dx.doi.org/10.1126/science.1175194

Zhang, S.Y., S. Boisson-Dupuis, A. Chapgier, K. Yang, J. Bustamante, A. Puel, C. Picard, L. Abel, E. Jouanguy, and J.L. Casanova. 2008. Inborn errors of interferon (IFN)-mediated immunity in humans: insights into the respective roles of IFN-α/β, IFN-γ, and IFN-λ in host defense. *Immunol. Rev.* 226:29–40. http://dx.doi.org/10.1111/j.1600-065X.2008.00698.x